A functional genetic toolbox for human tissue-derived organoids

Dawei Sun[1,2], Lewis Evans[3], Kyungtae Lim[1,4] and Emma L. Rawlins[1,4]

[1] Wellcome Trust/CRUK Gurdon Institute, University of Cambridge, Cambridge, CB2 1QN, UK.
[2] Department of Pathology, University of Cambridge, UK.
[3] Developmental Biology and Cancer Department, University College London, London, WC1N 1DZ, UK.
[4] Department of Physiology, Development and Neuroscience, University of Cambridge, UK.

Contact: e.rawlins@gurdon.cam.ac.uk

Key words: human, lung, organoids, CRISPR-Cas9, homologous gene targeting, inducible CRISPRi, CRISPRa, tetON, DHFR.

Abstract

Human organoid systems recapitulate key features of organs offering platforms for modelling developmental biology and disease. Tissue-derived organoids have been widely used to study the impact of extrinsic niche factors on stem cells. However, they are rarely used to study endogenous gene function due to the lack of efficient gene manipulation tools. We have systematically developed and optimised a complete genetic toolbox for tissue-derived organoids. This includes "Organoid Easytag", our efficient workflow for targeting all types of gene loci through CRISPR-mediated homologous recombination followed by flow cytometry for enriching correctly-targeted cells. Our toolbox also incorporates conditional gene knock-down, or overexpression, using tightly-inducible CRISPR interference and CRISPR activation; the first efficient application of these techniques to tissue-derived organoids. These tools will facilitate gene perturbation studies in tissue-derived organoids providing a functional counter-part to many on-going descriptive studies, such as the Human Cell Atlas Project.

Main

CRISPR and its related techniques (CRISPR interference and CRISPR activation, abbreviated as CRISPRi and CRISPRa) have transformed the study of gene function in model systems. They have been rapidly adopted in cancer and pluripotent stem cell (PSC) lines (Bowden et al., 2020; Gilbert et al., 2013; Tian et al., 2019), but not in tissue-derived human organoids. We have optimised these genetic tools for use in organoids using a tissue-derived human foetal lung organoid system (Nikolić et al., 2017).

First, we aimed to establish a robust workflow for gene targeting in organoids to facilitate reporter and direct knockout (KO) generation. A recent application of

30 non-homologous end joining (NHEJ) to improve gene targeting in organoids has
31 been successful (Artegiani et al., 2020). However, we adopted a homology
32 directed repair (HDR) strategy as a complementary approach. We reasoned that
33 the recombination-based method allows our strategy to deliver precise genetic
34 manipulation with flexible targeting sites and minimal additional genetic changes.
35 We chose fluorescence as a selection marker, allowing targeted cells to be easily
36 isolated using flow cytometry and chimeric colonies to be identified and removed
37 using a fluorescent microscope.
38
39 In order to achieve efficient gene targeting, we first sought to maximise: (1) the
40 efficiency of DNA delivery into organoid cells; (2) the efficiency of site-specific
41 DNA cleavage by the Cas9-gRNA complex. Nucleofection achieved up to 70%
42 transfection efficiency and showed consistency across different organoid lines
43 (Supplementary Fig. 1a, b). To optimize site-specific DNA cleavage, we used
44 nucleofection to introduce the Cas9-gRNA complex into cells in different forms
45 (Supplementary Fig. 1c). Consistent with previous reports Cas9 RNPs out-
46 performed plasmid based Cas9 approaches (Kim et al., 2014; Lin et al., 2014),
47 both in the T7 endonuclease assay and an online CRISPR editing analysis tool
48 (Supplementary Fig. 1c,d). Thus, we adopted nucleofection and ssRNP for
49 downstream experiments. This strategy has the advantage that the RNP is rapidly
50 degraded and should produce minimal off-target effects.
51
52 To establish our gene targeting workflow, we first focused on generating an
53 *ACTB*-fusion protein, taking advantage of the abundance of ACTB protein in
54 human foetal lung organoids and a previously-published targeting strategy
55 (Roberts et al., 2017). We designed a repair template to generate an N terminal
56 monomeric (m)*EGFP-ACTB* fusion (Fig. 1a). We set the following rules for
57 repair template design to facilitate efficient and consistent gene targeting: (1)
58 protospacer adjacent motif (PAM) sequence mutated to prevent editing by ssRNP

59 (Paquet et al., 2016); (2) 700 nt to 1000 nt length of each homologous arm (Yao
60 et al., 2018); (3) minimal plasmid size to maximise delivery into organoid cells;
61 (4) monomeric forms of fluorescent protein to avoid undesirable fusion protein
62 aggregates. As expected, 72 hours after nucleofection of the ssRNP and repair
63 template, mEGFP^{+} organoid cells could be enriched by flow cytometry (Fig. 1b,
64 c). These cells were collected and pooled together, but seeded sparsely, and
65 successfully expanded into organoid colonies (Fig. 1d). The mEGFP-ACTB
66 fusion protein localized to cell–cell junctions as expected (Roberts et al., 2017).
67 These small colonies could be further expanded into new organoid lines and 59%
68 of lines (n = 17/29 lines, from N = 2 parental organoid lines, Supplementary Fig.
69 5g) were correctly targeted. Targeted organoids continued to express the
70 multipotent lung progenitor marker, SOX9 (Fig. 1e). We sought to further
71 increase targeting efficiency using drugs previously reported to enhance HDR
72 (Maruyama et al., 2015; Song et al., 2016; Yu et al., 2015). However, using flow
73 cytometry as a simple assay, none of the drugs tested increased the rate of gene
74 targeting (Supplementary Fig. 2).
75
76 The *AAVS1* locus has been considered to be a 'safe harbour locus' for expressing
77 exogenous genes in a controllable manner in human cells without silencing
78 (Smith et al., 2008). As a further proof of concept, we successfully targeted
79 *AAVS1* to express a membrane tagged TagRFP-T (mTagRFP-T) for cell shape
80 visualisation (Fig. 1f, 1g). Therefore, we have combined Cas9 RNP with single-
81 stranded synthetic gRNA, a simple circular plasmid repair template and a strategy
82 to enrich correctly targeted cells via flow cytometry for gene targeting in human
83 foetal lung organoids. We named this workflow, Organoid Easytag.
84
85 To expand our Organoid Easytag pipeline to reporter generation we targeted
86 *SOX9*. SOX9, a transcription factor, is a tip progenitor cell marker for developing
87 lungs (Nikolić et al., 2017) and *SOX9* reporters are useful for monitoring organoid

88 progenitor state. To overcome its low expression level, we used a Histone H2B-
89 EGFP fusion (H2B-EGFP hereafter) to concentrate the EGFP signal in the
90 nucleus (Fig. 2a). A *T2A* sequence, a self-cleavage peptide, was also inserted
91 between *SOX9* and *H2B-EGFP*, to ensure that SOX9 protein was minimally
92 influenced. This strategy allowed us to enrich correctly targeted cells by flow
93 cytometry. Targeted colonies could be expanded and maintained normal SOX2,
94 SOX9 and NKX2-1 expression (Fig.2b; Supplementary Fig. 3d; Supplementary
95 Fig. 5g). Importantly, we noted that although we were only able to generate *SOX9*
96 reporter lines as heterozygotes (Supplementary Fig 3a, b), the gRNA sites in the
97 wildtype alleles were intact (6/6 lines tested, N=3 parental organoid lines)
98 (Supplementary Fig. 3c). This offers the opportunity to retarget the second allele
99 if desired.
100
101 We sought to apply Organoid Easytag to transcriptionally silent genes to generate
102 differentiation reporters. We adopted the strategy of inserting an exogenous
103 promoter flanked by two Rox sites which could be subsequently excised by Dre
104 recombinase (Anastassiadis et al., 2009; Roberts et al., 2019). The exogenous
105 *EF1a* promoter drives fluorescent reporter expression for flow cytometry
106 selection allowing us to first positively enrich correctly-targeted cells (Venus^{+}),
107 and subsequently enrich (Venus^{-}) cells following Dre-mediated *EF1a* removal
108 (Fig. 2c-2e; Supplementary Fig. 4). This design also helps to minimise the repair
109 template size. We targeted the *SFTPC* (surfactant protein C) and *TP63* genes,
110 because they are not expressed in human foetal lung organoid cells and they are
111 well established markers for alveolar type II and basal cell lineages respectively
112 (Barkauskas et al., 2013; Rock et al., 2009). To test *SFTPC* reporter function, we
113 overexpressed NKX2-1 from a lentiviral vector (Fig. 2f) (Attarian et al., 2018).
114 Following NKX2-1 induction, Venus was co-expressed with proSPTPC protein,
115 confirming that the reporter is functional (Fig. 2g). *TP63* reporter organoid lines

116 were produced using the same strategy (Supplementary Fig. 5). These results
117 indicate that the Organoid Easytag workflow can target silent gloci.
118
119 The generation of straightforward gene knockouts by induction of indels using
120 the CRISPR-Cas9 system can suffer from translation retention and exon skipping
121 (Smits et al., 2019; Tuladhar et al., 2019). Moreover, in the absence of a strong,
122 immediate phenotype the knockout cells cannot readily be identified. We sought
123 to solve these problems by generating a gene knockout in a controlled manner
124 using Organoid Easytag. We focused on *SOX2* as its function remains to be
125 elucidated in human foetal lung progenitors. We replaced the *SOX2* coding
126 sequence (CDS) with *T2A-H2B-EGFP* to generate *SOX2* knockout organoids.
127 Using two gRNAs targeting the N and C terminal of the *SOX2* CDS respectively,
128 we sequentially replaced both copies of the *SOX2* CDS (Fig. 2h; Supplementary
129 Fig. 6). The EGFP signal was increased after targeting the second copy of the
130 *SOX2* CDS, making selection of serially targeted alleles by flow cytometry
131 straightforward (Supplementary Fig. 6c). *SOX2* knockout colonies proliferate and
132 grow normally, suggesting that SOX2 is not crucial for human foetal lung tip
133 progenitor cell self-renewal (Fig. 2i).
134
135 We have demonstrated that our Organoid Easytag pipeline can target various loci,
136 including highly abundant genes, transcription factors, the human safe harbour
137 locus, transcriptionally silent genes and to generate knockouts (summarised in
138 Supplementary Fig. 5g).
139
140 Knockouts are not suitable for studying the function of genes which are required
141 for stem cell self-renewal. Moreover, temporal control of gene expression cannot
142 be easily achieved by knockouts. Inducible CRISPRi could potentially solve
143 these problems. We first embedded an N-terminal *KRAB-dCas9* fusion
144 (Mandegar et al., 2016) in a doxycycline (Dox) inducible TetON system aiming

145 to gain temporal control of CRISPRi function. However, the TetON system did
146 not provide tight control of CRISPRi (Supplementary Fig. 7). To solve the
147 leakiness problem we fused KRAB-dCas9 with a destabilising domain derived
148 from *E.coli* dihydrofolate reductase (DHFR) (Fig. 3a). DHFR is stabilised by a
149 small molecule, trimethoprim (TMP) (Fig. 3b) (Iwamoto et al., 2010). We
150 evaluated the new inducible CRISPRi system by depleting a ubiquitous cell
151 surface marker CD71 (Transferrin Receptor C, TFRC). Using previously
152 validated gRNAs (Horlbeck et al., 2016), CD71 protein was depleted in the
153 majority of the cells after 5 days of Dox and TMP treatment (91.4% ± 2.1%, mean
154 ± SEM, N =3 , Fig. 3c,d). Whereas no knockdown was observed in the no
155 Dox/TMP treatment group, or in organoids transduced with non-targeting control
156 gRNA. We further evaluated the inducible CRISPRi system using *SOX2*. SOX2
157 could be efficiently knocked down at both the transcriptional and protein level
158 and no leaky CRISPRi function was observed (Fig. 3e,f), indicating that CRISPRi
159 function has been tightly regulated. Consistent with our *SOX2* knockout (Fig. 2i),
160 we didn't observe effects on organoid morphology or growth after *SOX2*
161 knockdown (Fig. 3g,h). This further confirmed our finding that SOX2 is not
162 crucial for organoid self-renewal.
163
164 Finally, we have established the CRISPRa system to switch on endogenous genes
165 in human foetal lung organoids. We tested a previously reported CRISPRa system,
166 dxCas9(3.7)-VPR (Hu et al., 2018), for its ability to activate *SFTPC* transcription
167 (Fig. 4). Inducible CRISPRa can induce *SFTPC* gene expression efficiently at
168 both transcriptional and protein level without influencing organoid growth (Fig.
169 4b-d).
170
171 We have established a complete organoid genetic toolbox for gene targeting,
172 reporter generation, controllable gene knockouts, inducible gene knockdown and
173 gene activation in the human foetal lung organoid system. We envision that these

174 tools can be easily adapted for organoid systems derived from other tissues,
175 empowering tissue-derived organoids to benchmark gene function using the
176 Human Cell Atlas as a reference.

Acknowledgements

We thank Dr. Andrew Bassett (Wellcome Sanger Institute) for the Cas9 expressing vector. We thank Prof. Luke Gilbert (UCSF), Prof. Martin Kampmann (UCSF) and Prof. Ruilin Tian (SUSTech) for their advice on CRISPRi and CRISPRa.

D.S. is supported by a Wellcome Trust PhD studentship (109146/Z/15/Z) and the Department of Pathology, University of Cambridge; L.D.E is supported by the Alzheimer's Research UK Stem Cell Research Centre, funded by the Alborada Trust. K.L. is supported by Basic Science Research Program through the National Research Foundation of Korea (NRF) funded by the Ministry of Education (2018R1A6A3A03012122). E.L.R. is supported by Medical Research Council (MR/P009581/1). Core support from the Wellcome Trust (203144/Z/16/Z) and Cancer Research UK (C6946/A24843).

Contributions

D.S. designed and performed experiments, analysed data, wrote and edited the manuscript. L.D.E. performed experiments. K.L. performed experiments. E.L.R conceived and led the project, designed experiments, wrote and edited the manuscript.

207 **References**

208

209 **Anastassiadis, K., Fu, J., Patsch, C., Hu, S., Weidlich, S., Duerschke, K.,**
210 **Buchholz, F., Edenhofer, F. and Stewart, A. F.** (2009). Dre recombinase,
211 like Cre, is a highly efficient site-specific recombinase in E. coli,
212 mammalian cells and mice. *Dis Model Mech* **2**, 508–515.

213 **Artegiani, B., Hendriks, D., Beumer, J., Kok, R., Zheng, X., Joore, I.,**
214 **Chuva de Sousa Lopes, S., van Zon, J., Tans, S. and Clevers, H.** (2020).
215 Fast and efficient generation of knock-in human organoids using homology-
216 independent CRISPR-Cas9 precision genome editing. *Nat. Cell Biol.* **22**,
217 321–331.

218 **Attarian, S. J., Leibel, S. L., Yang, P., Alfano, D. N., Hackett, B. P., Cole, F.**
219 **S. and Hamvas, A.** (2018). Mutations in the thyroid transcription factor
220 gene NKX2-1 result in decreased expression of SFTPB and SFTPC. *Pediatr*
221 *Res* **84**, 419–425.

222 **Barkauskas, C. E., Cronce, M. J., Rackley, C. R., Bowie, E. J., Keene, D.**
223 **R., Stripp, B. R., Randell, S. H., Noble, P. W. and Hogan, B. L. M.**
224 (2013). Type 2 alveolar cells are stem cells in adult lung. *J. Clin. Invest.*
225 **123**, 3025–3036.

226 **Bowden, A. R., Morales-Juarez, D. A., Sczaniecka-Clift, M., Agudo, M. M.,**
227 **Lukashchuk, N., Thomas, J. C. and Jackson, S. P.** (2020). Parallel
228 CRISPR-Cas9 screens clarify impacts of p53 on screen performance. *Elife* **9**,
229 2430.

230 **Gilbert, L. A., Larson, M. H., Morsut, L., Liu, Z., Brar, G. A., Torres, S. E.,**
231 **Stern-Ginossar, N., Brandman, O., Whitehead, E. H., Doudna, J. A., et**
232 **al.** (2013). CRISPR-mediated modular RNA-guided regulation of

233 transcription in eukaryotes. *Cell* **154**, 442–451.

234 **Horlbeck, M. A., Gilbert, L. A., Villalta, J. E., Adamson, B., Pak, R. A.,**
235 **Chen, Y., Fields, A. P., Park, C. Y., Corn, J. E., Kampmann, M., et al.**
236 (2016). Compact and highly active next-generation libraries for CRISPR-
237 mediated gene repression and activation. *Elife* **5**, 914.

238 **Hu, J. H., Miller, S. M., Geurts, M. H., Tang, W., Chen, L., Sun, N., Zeina,**
239 **C. M., Gao, X., Rees, H. A., Lin, Z., et al.** (2018). Evolved Cas9 variants
240 with broad PAM compatibility and high DNA specificity. *Nature* **556**, 57–
241 63.

242 **Iwamoto, M., Björklund, T., Lundberg, C., Kirik, D. and Wandless, T. J.**
243 (2010). A General Chemical Method to Regulate Protein Stability in the
244 Mammalian Central Nervous System. *Chemistry & Biology* **17**, 981–988.

245 **Kim, S., Kim, D., Cho, S. W., Kim, J. and Kim, J.-S.** (2014). Highly efficient
246 RNA-guided genome editing in human cells via delivery of purified Cas9
247 ribonucleoproteins. *Genome Res.* **24**, 1012–1019.

248 **Lin, S., Staahl, B. T., Alla, R. K. and Doudna, J. A.** (2014). Enhanced
249 homology-directed human genome engineering by controlled timing of
250 CRISPR/Cas9 delivery. *Elife* **3**, e04766.

251 **Mandegar, M. A., Huebsch, N., Frolov, E. B., Shin, E., Truong, A., Olvera,**
252 **M. P., Chan, A. H., Miyaoka, Y., Holmes, K., Spencer, C. I., et al.**
253 (2016). CRISPR Interference Efficiently Induces Specific and Reversible
254 Gene Silencing in Human iPSCs. *Cell Stem Cell* **18**, 541–553.

255 **Maruyama, T., Dougan, S. K., Truttmann, M. C., Bilate, A. M., Ingram, J.**
256 **R. and Ploegh, H. L.** (2015). Increasing the efficiency of precise genome
257 editing with CRISPR-Cas9 by inhibition of nonhomologous end joining.

258 *Nat. Biotechnol.* **33**, 538–542.

259 **Nikolić, M. Z., Caritg, O., Jeng, Q., Johnson, J.-A., Sun, D., Howell, K. J.,**
260 **Brady, J. L., Laresgoiti, U., Allen, G., Butler, R., et al.** (2017). Human
261 embryonic lung epithelial tips are multipotent progenitors that can be
262 expanded in vitro as long-term self-renewing organoids. *Elife* **6**, e26575.

263 **Paquet, D., Kwart, D., Chen, A., Sproul, A., Jacob, S., Teo, S., Olsen, K.**
264 **M., Gregg, A., Noggle, S. and Tessier-Lavigne, M.** (2016). Efficient
265 introduction of specific homozygous and heterozygous mutations using
266 CRISPR/Cas9. *Nature* **533**, 125–129.

267 **Roberts, B., Haupt, A., Tucker, A., Grancharova, T., Arakaki, J., Fuqua,**
268 **M. A., Nelson, A., Hookway, C., Ludmann, S. A., Mueller, I. A., et al.**
269 (2017). Systematic gene tagging using CRISPR/Cas9 in human stem cells to
270 illuminate cell organization. *Mol. Biol. Cell* **28**, 2854–2874.

271 **Roberts, B., Hendershott, M. C., Arakaki, J., Gerbin, K. A., Malik, H.,**
272 **Nelson, A., Gehring, J., Hookway, C., Ludmann, S. A., Yang, R., et al.**
273 (2019). Fluorescent Gene Tagging of Transcriptionally Silent Genes in
274 hiPSCs. *Stem Cell Reports* **12**, 1145–1158.

275 **Rock, J. R., Onaitis, M. W., Rawlins, E. L., Lu, Y., Clark, C. P., Xue, Y.,**
276 **Randell, S. H. and Hogan, B. L. M.** (2009). Basal cells as stem cells of the
277 mouse trachea and human airway epithelium. *PNAS* **106**, 12771–12775.

278 **Smith, J. R., Maguire, S., Davis, L. A., Alexander, M., Yang, F., Chandran,**
279 **S., ffrench-Constant, C. and Pedersen, R. A.** (2008). Robust, persistent
280 transgene expression in human embryonic stem cells is achieved with
281 AAVS1-targeted integration. *Stem Cells* **26**, 496–504.

282 **Smits, A. H., Ziebell, F., Joberty, G., Zinn, N., Mueller, W. F., Clauder-**

283 **Münster, S., Eberhard, D., Savitski, M. F., Grandi, P., Jakob, P., et al.**
284 (2019). Biological plasticity rescues target activity in CRISPR knock outs.
285 *Nat. Methods* **16**, 1087–1093.

286 **Song, J., Yang, D., Xu, J., Zhu, T., Chen, Y. E. and Zhang, J.** (2016). RS-1
287 enhances CRISPR/Cas9- and TALEN-mediated knock-in efficiency. *Nat*
288 *Commun* **7**, 1–7.

289 **Tian, R., Gachechiladze, M. A., Ludwig, C. H., Laurie, M. T., Hong, J. Y.,**
290 **Nathaniel, D., Prabhu, A. V., Fernandopulle, M. S., Patel, R., Abshari,**
291 **M., et al.** (2019). CRISPR Interference-Based Platform for Multimodal
292 Genetic Screens in Human iPSC-Derived Neurons. *Neuron* **104**, 239–
293 255.e12.

294 **Tuladhar, R., Yeu, Y., Piazza, J. T., Tan, Z., Clemenceau, J. R., Wu, X.,**
295 **Barrett, Q., Herbert, J., Mathews, D. H., Kim, J., et al.** (2019). CRISPR-
296 Cas9-based mutagenesis frequently provokes on-target mRNA
297 misregulation. *Nat Commun* **10**, 1–10.

298 **Yao, X., Zhang, M., Wang, X., Ying, W., Hu, X., Dai, P., Meng, F., Shi, L.,**
299 **Sun, Y., Yao, N., et al.** (2018). Tild-CRISPR Allows for Efficient and
300 Precise Gene Knockin in Mouse and Human Cells. *Dev. Cell* **45**, 526–
301 536.e5.

302 **Yu, C., Liu, Y., Ma, T., Liu, K., Xu, S., Zhang, Y., Liu, H., La Russa, M.,**
303 **Xie, M., Ding, S., et al.** (2015). Small Molecules Enhance CRISPR Genome
304 Editing in Pluripotent Stem Cells. *Cell Stem Cell* **16**, 142–147.

305

306

307

308 **Methods**

309

310 **Derivation and maintenance of human foetal lung organoid culture**

311

312 Human foetal lung organoids were derived and maintained as previously reported
313 (Nikolić et al., 2017). Briefly, human foetal lung tissues were dissociated using
314 Dispase (8 U/ml Thermo Fisher Scientific, 17105041) at room temperature (RT)
315 for 2 min. Mesenchyme was dissected away using needles. Tips of the branching
316 epithelium were micro-dissected, transferred into 50 µl of Matrigel (356231,
317 Corning) and seeded in one well of a 24 well low-attachment plate (M9312-
318 100EA, Greiner). The plate was incubated at 37°C for 5 min to solidify the
319 Matrigel. 600 µl of self-renewing medium containing: N2 (1: 100), B27 (1: 50),
320 N-acetylcysteine (1.25 mM), EGF (50 ng/ml, PeproTech, AF-100-15), FGF10
321 (100 ng/ml, PeproTech, 100-26), FGF7 (100 ng/ml, PeproTech, 100-19), Noggin
322 (100 ng/ml, PeproTech, 120-10C), R-spondin (5% v/v, Stem Cell Institute,
323 University of Cambridge), CHIR99021 (3 µM, Stem Cell Institute, University of
324 Cambridge) and SB 431542 (10 µM, bio-techne, 1614), was added. The plate was
325 incubated under standard tissue culture conditions (37°C, 5% CO_2). Once formed,
326 organoids were maintained in self-renewing medium and passaged by
327 mechanically breaking using P200 pipettes every 10-14 days.

328

329 **Whole mount immunostaining for human foetal lung organoids**

330

331 Organoids were fixed with 4% paraformaldehyde (PFA) directly in the culture
332 plates on ice for 30 min. After two PBS washes, 0.5% (w/v) Bovine Serum
333 Albumin (BSA), 0.2% Triton-X in PBS (washing solution) was added and left on
334 ice overnight to dissolve Matrigel. Organoids were then transferred into multiple
335 CellCarrier-96 Ultra Microplates (PerkinElmer, 6055300) for staining.
336 Subsequently, blocking was performed in 5% donkey serum (Stratech, 017-000-

337 121-JIR), 0.5% (w/v) Bovine Serum Albumin (BSA), 0.2% Triton-X in PBS
338 (blocking solution) at 4°C overnight. For primary antibody staining, the
339 following antibodies in blocking solution were used at 4°C overnight: SOX2 (1:
340 500, Bio-techne, AF2018), SOX9 (1: 500, Sigma, AB5535), E-cadherin (1: 1500,
341 Thermo Fisher Scientific, 13-1900), NKX2-1 (1: 500, AbCam, ab76013),
342 TagRFP (1: 1000, Evrogen, AB233), GFP (1: 500, AbCam, ab13970), proSPC
343 (1: 500, Merck, AB3786). After washing off the primary antibodies, the
344 following secondary antibodies in washing buffer were used at 4°C overnight:
345 donkey anti-chick Alexa 488 (1: 2000, Jackson Immune, 703-545-155), donkey
346 anti-rabbit Alexa 594 (1: 2000, Thermo Fisher Scientific, A-21207), donkey anti-
347 goat Alexa 594 (1: 2000, Thermo Fisher Scientific, A-11058), donkey anti-goat
348 Alexa 647 (1: 2000, Thermo Fisher Scientific, A-21447), donkey anti-rat Alexa
349 647 (1: 2000, Jackson Immune, 712-605-153). The following day, DAPI (Sigma,
350 D9542) staining was performed in washing solution at 4°C for 30 min. After two
351 washes with PBS, 97% (v/v) 2'−2'-thio-diethanol (TDE, Sigma, 166782) in PBS
352 was used for mounting. Confocal z stacks were acquired using Leica SP8 at an
353 optical resolution of 1024 × 1024 using a 40x lens. Single plane images are shown.
354 Images were processed using ImageJ (version 2.0.0).
355
356 **Plasmid nucleofection**
357
358 For testing transduction efficiency, organoids were dissociated into single cells
359 using pre-warmed TrypLE™ Express (12605028, Thermo Fisher Scientific) at
360 37°C for 10 min. The reaction was terminated by adding Advanced DMEM/F12
361 (12634028, Thermo Fisher Scientific) and cells passed through a 30-micron cell
362 strainer. 2×10^5 organoid single cells were re-suspended with Lonza P3
363 nucleofection buffer and 1 μl of pmaxGFP (Lonza) and transferred to 20 μl
364 nucleofection cuvette (V4XP-3024, Lonza). Nucleofection was performed using
365 Lonza 4D Nucleofector with X unit using program EA125. After nucleofection,

366 self-renewing medium supplemented with 10 μM Y-27632 (ROCK inhibitor,
367 ROCKi, 688000, Merck) was added to dilute the P3 buffer. Cell mixture was then
368 seeded in Matrigel in 2 wells of a 24-well plate and cultured with self-renewing
369 medium with ROCKi (10 μM) for 72 hrs before FACS analysis.
370
371 **Lentiviral production**
372
373 We grew HEK293T cells in 10-cm dishes to a confluence of 80% before we
374 transfected the lentiviral vector (10 μg) with packaging vectors including
375 pMD2.G (3 μg, Addgene plasmid # 12259), psPAX2 (6 μg, Addgene plasmid #
376 12260) and pAdVAntage (3 μg, E1711, Promega) using Lipofectamine 2000
377 Transfection Reagent (11668019, Thermo Fisher Scientific) according to
378 manufacturer's protocol. After 16 hrs, medium was refreshed. Supernatant
379 containing lentivirus was harvested at 24 hrs and 48 hrs after medium refreshing
380 and pooled together. Supernatant was centrifuged at 300g to remove cell
381 fragments and passed through 0.45 μm filter. Lentivirus containing > 10 kb length
382 insert (inducible CRISPRi and CRISPRa) was concentrated using AVANTI J-30I
383 centrifuge (Beckman Coulter) with JS-24.38 swing rotor at 72000g for two hours
384 at 4 degree. Lentivirus pellets were dissolved in 200 μl PBS. Other Lentivirus,
385 including gRNA and NKX2-1 inducible overexpression, was concentrated using
386 Lenti-X™ Concentrator (631232, Takara). Lentivirus pellets were dissolved in
387 400 μl PBS.
388
389 **Lentivirus infection of organoids to test infection efficiency**
390
391 Organoid single cell suspension was prepared as for nucleofection. 5 μl lentivirus
392 (CMV-myrAKT-IRES-GFP) suspension was applied to 2×10^5 organoid single
393 cells suspended in 500 μl self-renewing medium with 10 μM ROCKi (without
394 Matrigel) in one well of 24-well plate and incubated at 37 °C overnight. The

395 following day, cells were harvested and washed twice with PBS before pelleting
396 and seeding in Matrigel in two wells of 24-well plate. Cells were grown in self-
397 renewing medium with ROCKi (10 μM) for 72 hrs before flow cytometry. CMV-
398 myrAKT-IRES-GFP was only used for checking lentiviral transduction
399 efficiency (Supplemental Fig. 1).
400
401 **Lipofectamine transfection of organoids**
402
403 Organoid single cells were prepared the same way as for nucleofection. For
404 comparing transduction efficiency, 1 μg of pmaxGFP (Lonza) was mixed with 1
405 μl of Lipofectamine™ Stem Transfection Reagent (STEM00001, Thermo Fisher
406 Scientific) according to manufacturer's protocol. 50 μl reaction mixture was
407 applied to 2×10^5 organoid single cells suspended with 450 μl self-renewing
408 medium with ROCKi (without Matrigel) in a single well of a 24-well plate. The
409 plate was then centrifuged at 32°C at 600g for 1 hr, followed by incubation at
410 37°C for 2-4 hrs. Cells were then harvested, pelleted and seeded in Matrigel in
411 two wells of a 24-well plate and grown in self-renewing medium supplemented
412 with ROCKi (10 μM) for 72 hrs before FACS analysis.

413
414 **Nucleofection for gene targeting**
415
416 Cas9 protein was prepared and used as previously reported (Bruntraeger et al.,
417 2019). If synthetic single strand gRNAs were used, 2 μl spCas9 (4 μg/μl) and 2.88
418 μl of ssRNA (100 μM, Synthego) were mixed and incubated at RT for a minimum
419 of 10 min in order to form ssRNPs. If synthetic cr/tr RNA heterodimers were used,
420 200 pmol synthetic cr RNA (IDT) and 200 pmol synthetic tr RNA (IDT) were
421 mixed with 2.5 μl Nuclease Free Duplex Buffer (11-01-03-01, IDT) and
422 denatured at 95 °C for 2 min. 2 μl of cr/tr RNA heterodimer was cooled down to

423 RT on the bench, mixed with 2 μl spCas9 (4 ug/ul) and incubated at RT for a
424 minimum of 10 min to form cr/tr RNPs. At the same time organoids were
425 dissociated into single cells, according to the protocol previously described for
426 nucleofection. 4×10^5cells were suspended using Lonza Nucleofection P3 buffer,
427 mixed with 10 μg of appropriate plasmid repair template, or with 500 pmol
428 ACTB-GFP11 ssODN (Ultramer DNA Oligos, IDT) with 5 μg CMV-GFP(1-10)
429 plasmid. The cell suspension was further mixed with pre-formed Cas9 RNPs and
430 equally distributed into two 20 μl cuvettes (V4XP-3024, Lonza). Nucleofection
431 was performed using program EA104. After nucleofection, self-renewing
432 medium with ROCKi was added to dilute the P3 buffer. Cell mixture was then
433 taken out and seeded in Matrigel in 4 wells of a 24-well plate and cultured with
434 self-renewing medium with 10 μM ROCKi for 72 hrs before flow cytometry.
435
436 gRNA sequences used for gene targeting are as follows:
437 *ACTB 5'-GCTATTCTCGCAGCTCACCA TGG*,
438 *SOX9 5'-CTTGAGGAGGCCTCCCACGA AGG*,
439 *AAVS1 5'-GTCCCCTCCACCCCACAGTG GGG*,
440 *SOX2 N terminal 5'-CGGGCCCGCAGCAAACTTCG GGG*,
441 *SOX2 C terminal 5'-CGGCCCTCACATGTGTGAGA GGG*.
442 *SFTPC 5'- GCGTCCTAGATGTAGTAGAG CGG*.
443 *TP63 5'- TGATGCGCTGTTGCTTATTG CGG*.
444 PAM sequences are underlined.
445
446 **Small molecule influence on gene targeting efficiency**
447
448 mEGFP-ACTB gene targeting was performed as previously described. After
449 nucleofection, DMSO (0.6 ul, D2650, Sigma), RS-1 (10 uM, R9782, Sigma),
450 L755507 (5 uM, SML1362, Sigma), or SCR-7 (100 uM, SML1546, Sigma) were

451 added to self-renewing medium with ROCKi for 48 hrs. Organoid cells were
452 analysed by flow cytometry 72 hrs after nucleofection.
453
454 **T7 Endonuclease Assay**
455
456 To test for site specific DNA cleavage using the T7 endonuclease assay, organoid
457 cells were harvested 48 hrs after nucleofection of ssRNP, tr/cr RNP, plasmid
458 encoding Cas9 and gRNA or WT control organoids. Genomic DNA was
459 extracted using QIAamp Fast DNA Tissue Kit (51404, Qiagen). PCR was
460 performed using PrimeSTAR® GXL DNA Polymerase (R050A, Takara) with 20
461 ng of genomic DNA as template according to manufacturer's protocol. Forward
462 primer: 5'-*TTGCCAATGGGGATCGCAG*-3' and reverse primer: 5'-
463 *GCTCGATGGGGTACTTCAGG*-3' were used for *ACTB* locus amplification. 10
464 µl of PCR product was then mixed with 1.5 µl 10X NEBuffer 2 (B7002S, NEB)
465 and 1.5 µl of Nuclease-free water. The mixture was denatured at 95°C for 10 min,
466 followed by ramp -2°C per second from 95°C to 85°C and ramp -0.3 °C per
467 second from 85°C to 25°C. 2 µl T7 Endonuclease I (1 U/ul, M0302S, NEB) was
468 added and incubated at 37°C for 1 hr. 2.5% Agarose gel was used for
469 electrophoresis.
470
471 **ICE analysis for Indel production**
472
473 Genomic DNA was extracted from organoid cells which were harvested 48 hrs
474 after nucleofection of ssRNP, tr/cr RNP, plasmid encoding Cas9 and gRNA or
475 WT control organoids using QIAamp Fast DNA Tissue Kit (51404, Qiagen).
476 PCR was performed using PrimeSTAR® GXL DNA Polymerase (R050A,
477 Takara) with 20 ng of genomic DNA as template according to manufacturer's
478 protocol. Forward primer: 5'-*TTGCCAATGGGGATCGCAG*-3' and reverse
479 primer: 5'-*GCTCGATGGGGTACTTCAGG*-3' were used for *ACTB* locus

480 amplification. PCR products were cleaned up using Macherey-Nagel™
481 NucleoSpin™ Gel and PCR Clean-up Kit (Macherey-Nagel, 740609.50) and sent
482 for Sanger Sequencing (Department of Biochemistry, University of Cambridge)
483 using reverse primer: 5'-*GCTCGATGGGGTACTTCAGG*-3'. Sanger sequencing
484 results were compared using ICE online CRISPR editing analysis tool:
485 https://www.synthego.com/products/bioinformatics/crispr-analysis
486
487 **Flow cytometry analysis**
488
489 Organoid single cells were prepared 72 hrs after nucleofection, lentivirus
490 transduction or Lipofectamine transfection. Cells were analysed using Sony
491 SH800S Cell Sorter and Flowjo software (version 10.4).
492

493 **Organoid Genotyping**

494 Organoids from a single 48-well plate well were used for genomic DNA
495 extraction with QIAamp Fast DNA Tissue Kit (51404, Qiagen) according to
496 manufacturer's protocol. PCR was performed using PrimeSTAR® GXL DNA
497 Polymerase (R050A, Takara) with 20 ng of genomic DNA as template according
498 to manufacturer's protocol. Primers used are listed in genotyping primers file.
499 For each gene targeting, 3 randomly picked lines were chosen for further Sanger
500 Sequencing. 5' and 3' homologous arms of the gene targeting product were
501 amplified using PrimeSTAR® GXL DNA Polymerase with aforementioned
502 primers. PCR products were cleaned up using Macherey-Nagel™ NucleoSpin™
503 Gel and PCR Clean-up Kit (Macherey-Nagel, 740609.50) and sequenced using
504 Sanger Sequencing (Department of Biochemistry, University of Cambridge).
505
506 **Western blot**

507

508 Organoids were harvested, washed twice with Advanced DMEM/F12 and then
509 twice with PBS before pelleting at 300g for 5 min. Organoid cell pellets were re-
510 suspended in 100 µl-200 µl of RIPA buffer with protease inhibitor (Thermo
511 Fisher Scientific, 87786) added. Organoid suspension was incubated for 30
512 minutes on ice, with strong vortex every 5 minutes. Cell pieces and debris were
513 removed by centrifugation at 13000 rpm. Supernatant was harvested. Protein
514 concentration was measured by BCA assay (Thermo Fisher Scientific, 23227).
515 Equal amount of each protein sample was mixed with Sample Buffer (Bio-rad,
516 1610747) and beta-mercaptoethanol according to manufacturer's protocol.
517 Mixture was heated at 95 °C for 5 minutes and cooled down to room temperature.
518

519 Samples were then separated on a 4%–12% SDS-PAGE and transferred to
520 nitrocellulose membranes. Membrane was blocked by PBS with 5% BSA for 1
521 hour at room temperature. Proteins were detected by incubation with primary
522 antibodies (SOX2, Bio-techne, AF2018, 1: 1000 and α-Tubulin, Merck, T6199,
523 1:2000) and secondary antibodies (Donkey anti-Goat IRDye® 800CW, AbCam,
524 ab216775, 1: 1000; Donkey anti-Mouse IRDye® 800CW, ab21677, 1: 1000).
525 Protein bands were visualised using Li-Cor Odyssey system.
526

527 **Lentivirus infection of organoids for inducible knockout and activation**
528

529 Organoids were dissociated into small organoid pieces or single cells using pre-
530 warmed TrypLE™ Express at 37°C for 5-10 min. Organoid cells were then spun
531 down at 300g for 5 min. The cell pellets from one 24-well-plate well were
532 responded in 500µl self-renewing medium with ROCKi. 20ul of inducible
533 CRISPRi or CRISPRa lentivirus was added and mixed well. The mixture was
534 incubated at 37 degree overnight. The next morning, organoid cells were pelleted
535 at 300g for 5 min, washed twice with PBS and seeded in 100µl Matrigel into 2

536 24-well-plate wells. Organoid cells were cultured with self-renewing medium
537 with ROCKi for 3 days before dissociated with TrypLE™ Express into single
538 cells for cell sorting. TagRFP^{+} cells were sorted using Sony SH800S Cell Sorter
539 and pooled together and seeded in Matrigel at approx. 3000-5000 cells/well of a
540 24-well plate. Organoids cells were then expanded around 17 days using self-
541 renewing medium with ROCKi. At this stage, organoids with inducible CRISPRi
542 and CRISPRa system could be frozen as parental lines.
543
544 Organoids with inducible CRISPRi and CRISPRa system were broken into small
545 organoid pieces or single cells similarly and transduced with gRNA lentivirus
546 (5µl-10µl virus/500µl organoid cell resuspension). The mixture was incubated
547 overnight and the next morning, organoid cells were pelleted, washed and seeded
548 with Matrigel as described above. After 3 days of culturing with self-renewing
549 medium supplemented with ROCKi, TagRFP and EGFP double positive cells
550 were sorted and seeded in Matrigel at approx. approx. 2000-3000 cells/well of a
551 24-well plate and expanded for 10-17 days before turning on inducible CRISPRa
552 and CRISPRi. Doxycycline (2 µg/ml, Merck, D9891) and trimethoprim (10
553 nmol/L, Merck, 92131) were supplemented in self-renewing medium accordingly.
554 Medium was refreshed every 48 hours.
555
556 For evaluation of inducible CRISPRi using *CD71* as target, single cells were
557 prepared as described above after 5 days of Dox and TMP treatment. Cells were
558 pelleted at 300g for 5min and re-suspended in 100 µl PBS with 0.5%BSA and
559 2mM EDTA. 2.5 µl of PE/Cy7 anti-human CD71 antibody (BioLegend, 334111)
560 was added and incubated at 4 degree for 30 min. Cells were then washed with
561 PBS with 0.5%BSA and 2mM EDTA twice and re-suspended in 300 µl of PBS
562 with 0.5%BSA and 2mM EDTA for flow cytometry analysis.
563
564 **RNA extraction, cDNA synthesis and qRT-PCR**

565

566 Organoids were harvested and washed twice with Advanced DMEM/F12, before
567 350 µl of RLT buffer was added to lyse organoids. RNA extraction was
568 performed according to manufacturer's protocol using RNeasy Mini Kit (Qiagen,
569 74104) with RNase-Free DNase Set (Qiagen, 79254). RNA concentrations were
570 measured by Nanodrop (Thermo Fisher Scientific). cDNA was synthesized with
571 MultiScribe™ Reverse Transcriptase (Thermo Fisher Scientific, 4311235)
572 according to manufacturer's protocol. cDNA was diluted 1: 25 and 6 µl was used
573 for one qPCR reaction with PowerUp™ SYBR™ Green Master Mix (Thermo
574 Fisher Scientific, A25776). Relative gene expression was calculated using the
575 ΔΔCT method relative to *ACTB* control.

576

577 **Plasmid Construction**

578 eSpCas9(1.1) was a gift from Feng Zhang (Addgene plasmid # 71814). ACTB
579 gRNA sequence 5'-GCTATTCTCGCAGCTCACC-3' was cloned into the vector
580 using BbsI sites. ACTB repair template AICSDP-15: ACTB-mEGFP was a gift
581 from The Allen Institute for Cell Science (Addgene plasmid # 87425). SOX9
582 repair template was created by Infusion (638909, Takara) cloning to insert SOX9
583 5' and 3' homologous arms in EasyFusion T2A-H2B-GFP plasmid (a gift from
584 Janet Rossant, Addgene plasmid # 112851). AAVS1 repair template was created
585 by Infusion cloning to swap the CAG promoter and Puromycin resistance cassette
586 in plasmid AICSDP-42: AAVS1-mTagRFPT-CAAX (a gift from The Allen
587 Institute for Cell Science, Addgene plasmid # 107580). SOX2 knockout repair
588 template was created by Infusion cloning to insert SOX2 5' and 3' homologous
589 arms in EasyFusion T2A-H2B-GFP (a gift from Janet Rossant, Addgene plasmid
590 # 112851). SFTPC targeting repair template was created by Infusion assembly of
591 SFTPC 5' and 3' homologous arms together with T2A-Rox-EF1a-Rox-Venus-
592 NLS. TP63 targeting repair template was created by Infusion assembly of TP63

593 5’ and 3’ homologous arms together with T2A-Rox-EF1a-Rox-Venus-NLS.
594 CMV-Dre-T2A-TagRFP vector was created by Infusion assembly of Dre (a gift
595 from Azim Surani Group, Gurdon Institute, Cambridge) and T2A-TagRFP
596 sequences together. NKX2-1 overexpression vector was created by inserting
597 EF1a-TagRFP-2A-tet3G and tetON-NKX2-1 CDS in 2 steps cloning using
598 Infusion cloning into a pHAGE backbone. The minimal CMV-GFP(1-10)
599 plasmid was created by Infusion cloning of CMV-GFP(1-10) from pcDNA3.1-
600 GFP(1-10) (a gift from Bo Huang (Addgene plasmid # 70219) into a pUC57
601 backbone. For testing lentiviral transduction efficiency, CMV-myrAKT-IRES-
602 GFP vector was created by Infusion cloning to insert myrAKT from pCCL-Akt1
603 (a gift from Bi-Sen Ding, Icahn School of Medicine, Mount Sinai) and IRES
604 sequence into pFP945 (a gift from Frederick Livesey, University College
605 London). The Dox inducible CRISPRi vector was created by sub-cloning N-
606 terminal KRAB-dCas9 (a gift from Bruce Conklin, Addgene plasmid # 73498)
607 into the NKX2-1 overexpressing vector using XhoI and BamHI sites. Dox
608 inducible CRISPRi with DD control vector was created by In-fusion cloning of a
609 C-terminal DHFR sequence into the Dox inducible CRISPRi vector using BamHI
610 site. The inducible CRISPRa vector was created by sub-cloning dxCas9(3.7)-
611 VPR (a gift from David Liu, Addgene plasmid # 108383) into the NKX2-1
612 overexpressing vector using XhoI and BamHI sites. The gRNA entry vector was
613 cloned by infusion cloning of a EF1a promoter into pKLV2-U6gRNA5(BbsI)-
614 PGKpuro2ABFP-W vector (a gift from Kosuke Yusa, Addgene plasmid # 67974)
615 using BamHI and EcoRI sites, and then cloned a EGFP-CAAX to swap the EGFP
616 sequence using XhoI and NotI sites. All plasmids will be deposited in Addgene.
617
618
619
620
621

622 **Figure Legends**

623

624 **Figure 1. The Organoid Easytag workflow for gene targeting in human**
625 **organoids. (a)** Schematic of the Organoid Easytag workflow. ssRNP and a
626 circular plasmid repair template are nucleofected into dissociated cells at day 0.
627 By day 3 cells have proliferated to become tiny colonies and are removed from
628 the Matrigel and dissociated for selection by flow cytometry. $EGFP^+$ cells are re-
629 plated sparsely (approx. 1000-1500 cells/well of a 24-well plate) and grown until
630 day 15 when organoids reach a sufficient size to be manually picked under a
631 fluorescent microscope. Organoids are picked into individual wells and passaged
632 until sufficient cells are obtained for both genotyping and freezing down the line.
633 Cells with red nuclei represent incorrectly targeted cells. Cells with white nuclei
634 denote correctly targeted cells. **(b)** Schematic of repair template design for N
635 terminal fusion *mEGFP-ACTB* gene targeting and the final product. Arrow shows
636 the position of gRNA. E1, exon 1; E2, exon 2; 5'HA, 5' homology arm; 3'HA, 3'
637 homology arm. **(c)** Representative flow cytometry results showing the percentage
638 of EGFP cells 72 hrs after nucleofection is performed. **(d)** Representative image
639 showing *mEGFP-ACTB* organoid. DIC channel on the left and EGFP channel on
640 the right. **(e)** Immunofluorescence of *mEGFP-ACTB* organoids. Blue: DAPI
641 (nuclei); green: EGFP (ACTB fusion protein); red: SOX9 (lung progenitor
642 marker). (**f**) Schematic of the *AAVS1* targeting repair template design and the final
643 product. E1: Exon1. E2: Exon 2. Arrow indicates the position of the gRNA. **(g)**
644 Immunofluorescence of *AAVS1-EF1a-mTagRFP-T* organoids. Blue: DAPI
645 (nuclei); red: mTagRFP-T (membrane localised reporter); white: SOX2 (lung
646 progenitor marker). Scale bars in all panels denote 50 μm.

647

648

649 **Figure 2. Organoid Easytag workflow facilitates reporter generation and**
650 **direct knockouts. (a)** Schematic of the *SOX9* locus repair template design and

651 final product. E1, Exon 1; E2, Exon 2; E3, Exon 3. 5' HA, 5' homology arm; 3'
652 HA, 3' homology arm. Arrow shows the position of the gRNA. **(b)**
653 Immunofluorescence of *SOX9-T2A-H2B-EGFP* organoids. Green: EGFP (SOX9
654 reporter); red: SOX9 (lung progenitor marker); white: ECAD (E-cadherin, basal-
655 lateral junctions). **(c)** Strategy for targeting transcriptionally silent genes using
656 the Organoid Easytag workflow. First step: knocking-in to the 3' end of the locus
657 an exogenous *EF1a* promoter, which is flanked by two Rox sites, driving nuclear-
658 localised Venus expression. A T2A peptide sequence is inserted before the *EF1a*
659 promoter in order to minimise the influence of the future fluorescent reporter on
660 the gene of interest (GOI). Second step: Transient transfection of a plasmid
661 encoding the Dre-recombinase to remove the exogenous *EF1a* promoter. This
662 results in Venus expression becoming dependent on transcription of the targeted
663 locus. (**d**) Schematic of the *SFTPC* locus repair template design and final product.
664 E5, Exon 5; 5' HA, 5' homology arm; 3' HA, 3' homology arm. Arrow indicates
665 the position of the gRNA. Red bar indicates the position of the stop codon. (**e**)
666 Representative images showing *SFTPC-T2A-Rox-EF1a-Rox-Venus-NLS*
667 organoids before and after Dre recombinase expression. Upper panel: nuclear
668 localised Venus fluorescence can be observed under a standard epifluorescent
669 microscope before Dre recombinase expression; bottom panel: Venus fluorescent
670 signal is lost after Dre recombinase expression. Arrows indicate nuclear localised
671 Venus signal. **(f)** Schematic of the strategy for testing *SFTPC* reporter function
672 by NKX2-1 overexpression. *SFTPC* reporter lines were dissociated and
673 transduced with NKX2-1 conditional overexpression lentivirus. Transduced cells
674 are marked by TagRFP expression which can be enriched via flow cytometry.
675 TagRFP expression is coupled to tet3G which, upon doxycycline (Dox)
676 administration, binds to the tetON promoter and drives NKX2-1 overexpression.
677 (**g**) Representative immunofluorescence showing that the *SFTPC* reporter is
678 functional. Blue: DAPI (nuclei); green: Venus (SFTPC reporter); white:
679 proSFTPC protein. (**h**) Schematic showing repair template design and final

680 product for the generation of *SOX2* knockout organoids using Organoid Easytag.
681 Two gRNA sites were used at the N and C terminal of the *SOX2* CDS respectively.
682 *SOX2* CDS was replaced by *T2A-H2B-EGFP*. (**i**) Representative
683 immunofluorescence showing that SOX2 protein is completely knocked-out.
684 Blue: DAPI (nuclei); green: EGFP (*SOX2* transcriptional reporter); red: SOX2
685 protein (lung progenitor marker); white: ECAD (E-cadherin, basal-lateral
686 junctions). Scale bars denote 50 μm (b, g) and 100 μm (e, i).
687
688 **Figure 3. Precise temporal control of CRISPRi in human foetal lung**
689 **organoids can be achieved via combining the Dox inducible system with a**
690 **protein destabilising domain. (a)** Schematic of lentiviral vector designs for
691 sequential introduction of inducible CRISPRi and gRNAs into human foetal lung
692 organoids. N-terminal KRAB-dCas9 was fused with DHFR derived destabilising
693 domain (DD) for stringent control of CRISPRi function. EGFP was fused with a
694 C-terminal CAAX domain to achieve membrane labelling of the transduced cells.
695 **(b)** Schematic showing how the temporal control of CRISPRi protein is achieved
696 by combining the Dox inducible system and DD. The Dox inducible system is
697 somewhat leaky, but in the absence of TMP, any KRAB-dCas9-DHFR fusion
698 protein produced is degraded. Dox treatment results in high levels of KRAB-
699 dCas9-DHFR fusion protein expression. When TMP is not present, the fusion
700 protein is destabilised, whereas when TMP is supplemented, the fusion protein is
701 stabilised and can exert its gene expression repression function. **(c)** Workflow for
702 generating gene knockdown (KD) using CRISPRi system. A parental organoid
703 line with inducible CRISPRi was introduced via lentiviral transduction followed
704 by sorting for TagRFP positive cells. Single cells were re-plated (approx. 3000-
705 5000 cells/well of a 24-well plate) and expanded for around 17 days. gRNA
706 lentivirus was then introduced by a second lentiviral transduction event, followed
707 by sorting for TagRFP/EGFP dual positive cells after 3 days. Cells were re-plated
708 again (approx. 2000-3000 cells/well of a 24-well plate) and expanded for another

709 10 days before treatment with Dox and TMP. 4-6 days after Dox and TMP
710 treatment gRNA performance was evaluated. **(d)** Representative flow cytometry
711 results for validation of inducible CRISPRi performance using CD71 as target.
712 After TMP and Dox administration for 5 days, CD71 protein was successfully
713 down-regulated. Grey histogram indicates CD71 expression level for organoids
714 with non-targeting control gRNA after Dox and TMP treatment for 5 days; blue
715 histogram indicates the CD71 expression level for organoids with CD71 gRNA
716 without Dox or TMP treatment, showing no KD effect; pink histogram indicates
717 the CD71 expression level for CD71 gRNA with Dox and TMP treatment for 5
718 days. **(e)** *SOX2* can be effectively knocked-down using inducible CRISPRi
719 without leaky effect indicated by qRT-PCR. Organoids with Dox and TMP
720 treatment were harvested 5 days after the treatment. Each dot represents an
721 independent experiment. 2 independent organoid lines with 2 different non-
722 targeting control gRNAs and 3 different SOX2 gRNAs were used. *SOX2*
723 expression level was normalised to organoids with non-targeting control (NT)
724 gRNAs. Detailed breakdown of these data is shown in Supplementary Figure 8(a).
725 Error bars are plotted to show mean ± SEM. A two-sided Student's t-test with
726 non-equal variance was used to compare the means of each group. * indicates p-
727 value < 0.05. n.s. indicates non-significant. **(f)** Representative western blot results
728 showing SOX2 was effectively knocked-down using the inducible CRISPRi
729 system. **(g-h)** Representative images showing organoid morphology after *SOX2*
730 knockdown. Images were taken after 5 days of Dox and TMP treatment. *SOX2*
731 knockdown (right panel) didn't result in obvious phenotypic changes in organoids
732 compared with non-targeting (NT) gRNA control (left panel). Scale bars denote
733 100 μm.
734
735 **Figure 4. Inducible CRISPRa induced silent gene, *SFTPC*, expression in**
736 **human foetal lung organoids. (a)** Schematic of lentiviral design for introducing
737 the CRISPRa system and gRNA into human foetal lung organoids. **(b)**

738 Representative images to show organoid morphology after *SFTPC* activation
739 after 6 days of Dox treatment. *SFTPC* activation (lower panel) didn't result in
740 obvious phenotypic changes in organoids compared with non-targeting gRNA
741 control (upper panel). **(c)** *SFTPC* can be effectively activated by CRISPRa system
742 indicated by qRT-PCR. Each dot represents an independent experiment. 2
743 independent organoid lines with 2 different non-targeting control (NT) gRNAs
744 and 3 different *SFTPC* gRNAs were used. *SFTPC* expression level was
745 normalised to organoids with non-targeting control (NT) gRNAs. A detailed
746 breakdown of the results is in Supplementary Figure 8(b). Error bars are plotted
747 to show mean ± SEM. A two-sided Student's t-test with non-equal variance was
748 used to compare the means of each group. ** indicates p-value < 0.01. **(d)**
749 Representative immunofluorescence showing proSFTPC protein accumulation in
750 organoid cells after CRISPRa activation of *SFTPC* gene expression. Bright
751 SFTPC protein aggregates accumulated in cells, consistent with the hydrophobic
752 nature of SFTPC protein. Green: EGFP. White: proSFTPC protein. Scale bars
753 denote 100 μm (b) and 50 μm (d).
754
755 **Supplementary Figure 1. Optimisation of DNA delivery and CRISPR**
756 **cutting. (a)** Efficiency quantification of different DNA delivery methods. EGFP
757 positive cells were quantified by flow cytometry 72 hrs after transfection or
758 transduction. N = 4 different organoid lines were used for each condition. Error
759 bars are plotted to show mean ± SEM. **(b)** Representative images showing DNA
760 delivery efficiencies of different methods 72 hrs after transfection/transduction.
761 Top panel: wide-field images; bottom panel: GFP channel. Scale bar denotes 100
762 μm. **(c)** T7 endonuclease assay showing the DNA cleavage efficiency of different
763 CRISPR methods on the *ACTB* locus. Arrows denote lower bands generated by
764 T7 endonuclease cutting. Left panel: schematic showing the different methods
765 tested for introducing the Cas9 complex. cr/tr RNP, synthetic crispr/tracer RNA
766 heterodimer with Cas9 RNP. ssRNA, single strand synthetic guide RNA with

767 Cas9 RNP. **(d)** Quantification of indels produced by the different CRISPR
768 methods tested using ICE online analysis software (https://ice.synthego.com/). N
769 =3 different organoid lines were used for each condition. Error bars are plotted to
770 show mean ± SEM.
771
772 **Supplementary Figure 2. Small molecules did not significantly improve**
773 **organoid gene targeting efficiency. (a)** Workflow for testing different HDR
774 enhancing drugs. Organoid cells were treated with DMSO, RS-1, L755507 and
775 SCR-7 for 48hrs after nucleofection for *mEGFP-ACTB* gene targeting. The
776 percentage of EGFP positive cells was analyzed 72 hrs after nucleofection.
777 DMSO treatment was used as a negative control. (**b**) Summary of percentage of
778 EGFP positive. No significant improvement of targeting efficiency was observed
779 after the drug treatments. N =3 different organoid lines were used. Error bars are
780 plotted to show mean ± SEM.
781
782
783 **Supplementary Figure 3. Characterisation of *SOX9* targeted colonies. (a)**
784 Immunofluorescence of a *SOX9-T2A-H2B-EGFP* clone. Blue: DAPI (nuclei);
785 green: H2B-EGFP (*SOX9* transcriptional reporter); red: NKX2-1 (lung epithelial
786 marker); white: SOX2 (lung progenitor marker). Scale bar denotes 50 μm. **(b)**
787 Schematic of the *SOX9* genotyping strategy. 5' and 3' junction amplicons consist
788 of a primer inside the EGFP sequence and another primer upstream, or
789 downstream, of the homology arm respectively. **(c)** Representative gel image
790 showing correct colony genotyping results. **(d)** Illustration of Sanger sequencing
791 results for *SOX9-T2A-H2B-EGFP* heterozygous WT allele, focusing on the
792 gRNA cutting sites. A single point mutation outside the gRNA sequence in the
793 3'UTR of SOX9 is observed in 4/6 of the clones sequenced (#3-#6). Results were
794 from 6 colonies, randomly picked from N = 3 different organoid lines.
795

796 **Supplementary Figure 4. Organoid Easytag to target the *SFTPC* locus. (a)**
797 Schematic of the *SFTPC* reporter genotyping strategy. 5' and 3' junction
798 amplicons consist of a primer inside the Venus sequence and another primer
799 upstream, or downstream, of the homology arm respectively. (**b**) Representative
800 gel image showing correct and incorrect colony genotyping results. Clone #10
801 was correctly targeted; Clone #6 appeared correctly targeted in gel, however,
802 Sanger sequencing revealed a deletion in the T2A sequence. Clone #1 and #5
803 were incorrectly targeted. **(c)** Representative flow cytometry results showing loss
804 of the Venus signal after transient expression of Dre recombinase to excise the
805 *EF1a* promoter. **(d)** Schematic of the final *SFTPC* reporter genotyping strategy
806 to validate *EF1a* removal. 5' and 3' junction amplicons consist of a primer inside
807 the Venus sequence and another primer upstream, or downstream, of the
808 homology arm respectively. **(e)** Representative gel image showing correct SFTPC
809 reporter colony (after Dre recombinase) genotyping results. **(f)** Sanger
810 Sequencing traces showing the correct *SFTPC-CDS-T2A* and *Venus-SFTPC*
811 3'UTR junctions.
812
813 **Supplementary Figure 5. Organoid Easytag to target the *TP63* locus. (a)**
814 Schematic of the *TP63* locus repair template design and final product. E14, Exon
815 14; 5' HA, 5' homology arm; 3' HA, 3' homology arm. Arrow indicates the
816 position of the gRNA. **(b)** Representative images showing *TP63-T2A-Rox-EF1a-*
817 *Rox-Venus-NLS* heterozygous organoid. Nuclear localised Venus fluorescence
818 can be observed under epifluorescent microscope. Scale bar indicates 50 µm. **(c)**
819 Schematic of the *TP63* genotyping strategy. 5' and 3' junction amplicons consist
820 of a primer inside the Venus sequence and another primer upstream, or
821 downstream, of the homology arm respectively. The expected lengths of each
822 amplicon are labelled below the schematic. **(d)** Representative gel image showing
823 correct colony genotyping results. The WT bands were excised for Sanger
824 sequencing in lanes #3. **(e)** Schematic of the final *TP63* reporter genotyping

825 strategy to validate *EF1a* removal. **(f)** Representative gel image showing correct
826 colony genotyping results after Dre recombinase. (**g**) Summary of all the gene
827 targeting results. For *SFTPC* and *TP63* reporter generation, results for the first
828 step gene targeting were shown. The number of lines that were generated after
829 Dre recombinase expression is shown in brackets.
830
831 **Supplementary Figure 6. Generation of *SOX2* knockout using organoid**
832 **Easytag workflow. (a)** Genotyping strategy for *SOX2 +/H2B-EGFP*
833 heterozygotes. **(b)** Representative gel image showing correctly targeted colonies.
834 **(c)** Representative flow cytometry results showing the EGFP signal shift from
835 WT control to *SOX2 +/H2BEGFP* Clone #5 heterozygote and *SOX2*
836 *+/H2BEGFP* Clone #5 retargeted to replace the second copy of the *SOX2 CDS*.
837 **(d)** Genotyping strategy for testing whether the WT *SOX2 CDS* is still present.
838 **(e)** Representative gel image showing correctly targeted colonies (Clone #5 and
839 # 6) with no amplification for WT *SOX2 CDS* in contrast to WT control.
840
841 **Supplementary Figure 7. The tetON system alone was not able to tightly**
842 **control CRISPRi function. (a)** Schematic of lentiviral design for introducing
843 inducible CRISPRi and gRNA into human foetal lung organoids. **(b)**
844 Representative images showing an organoid colony with both the inducible
845 CRISPRi system and a gRNA. Scale bar denotes 50 μm. **(c)** Workflow for testing
846 the leakiness of the inducible CRISPRi system. A parental organoid line with
847 inducible CRISPRi was introduced via lentiviral transduction, followed by
848 sorting for TagRFP positive cells. Single cells were re-plated (approx. 3000-5000
849 cells/well of a 24-well plate) and expanded for around 17 days. gRNA lentivirus
850 was then introduced by a second lentiviral transduction event, followed by sorting
851 for TagRFP/EGFP dual positive cells after 3 days. Cells were re-plated again
852 (approx. 2000-3000 cells/well of a 24-well plate) and expanded for another 10
853 days before treatment with Dox. 4-6 days after Dox treatment, gRNA

854 performance was evaluated. **(d)** *SOX2* can be effectively knocked-down by
855 inducible CRISPRi. However, the knockdown effect cannot be tightly controlled.
856 Organoids with Dox were harvested 4-6 days after the treatment. *SOX2* was
857 effectively knockdown at the mRNA level. However, a similar effect was
858 observed without Dox treatment. Each dot represents an independent experiment.
859 2 independent organoid lines with 2 different non-targeting control gRNAs and 3
860 different SOX2 gRNAs were used. SOX2 expression level was normalised to
861 organoids with non-targeting control gRNAs. Error bars are plotted to show mean
862 ± SEM. A two-sided Student's t-test with non-equal variance was used to compare
863 the means of each group. ** indicates p-value < 0.01. n.s. indicates non-
864 significant.
865
866 **Supplementary Figure 8 *SOX2* CRISPRi and *SFTPC* CRISPRa results**
867 **break down. (a)** qRT-PCR result details for Figure 3 (e). Each dot represents an
868 independent experiment. 2 independent organoid lines were used for each gRNAs.
869 *SOX2* expression levels were normalised to SOX2 expression level in organoids
870 with non-targeting (NT) control gRNA #1. Lines indicate means. **(b)** qRT-PCR
871 result details for Figure 4 (c). Each dot represents an independent experiment.
872 *SFTPC* expression levels were normalised to *SFTPC* expression level in
873 organoids with non-targeting (NT) control gRNA #1. 1 or 2 independent organoid
874 lines were used for each gRNAs. Lines indicate means.

Figure 1. The Organoid Easytag workflow for gene targeting in human organoids.

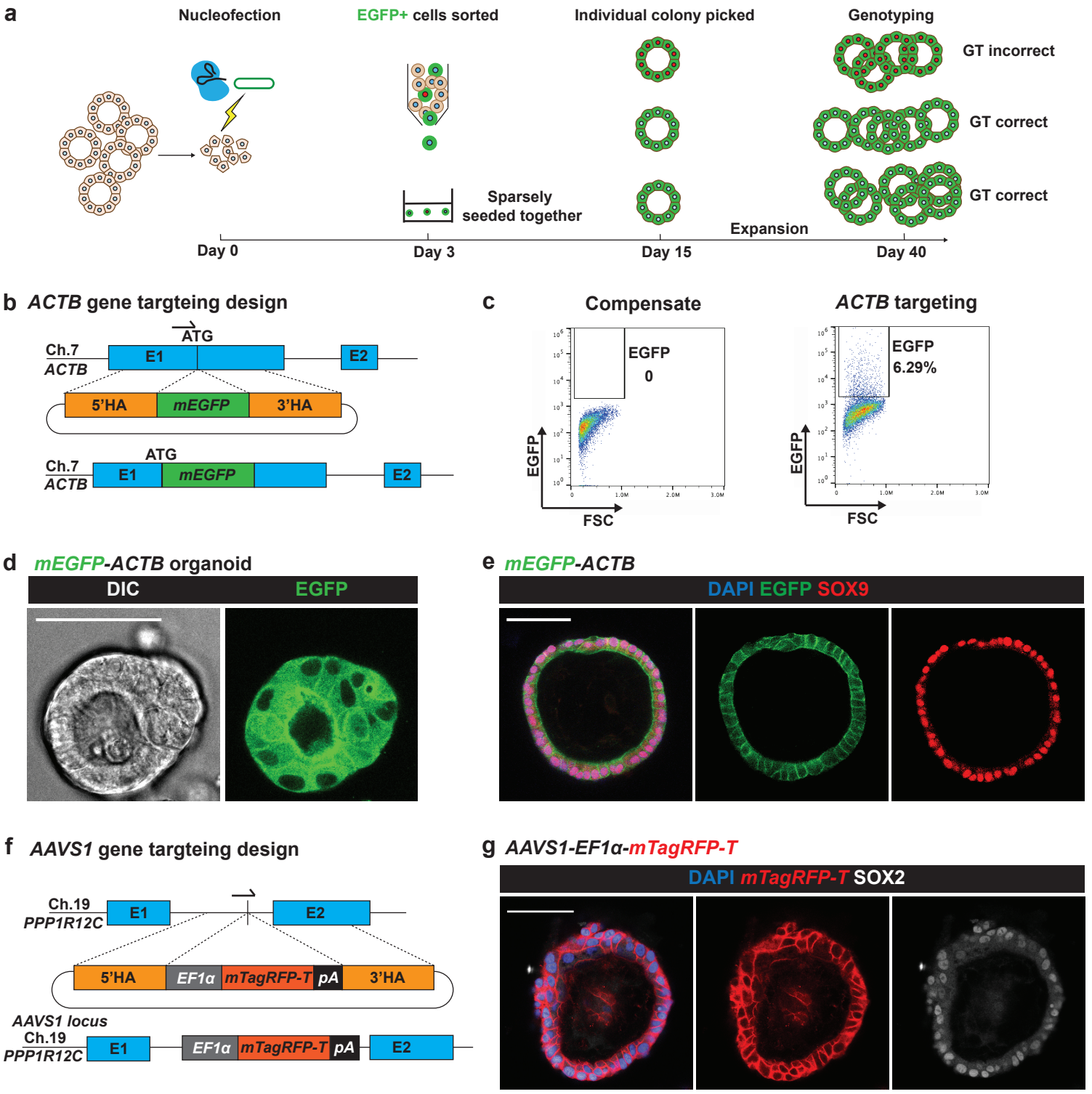

Figure 2. Organoid Easytag workflow facilitates reporter generation and direct knockouts.

a *SOX9* reporter design

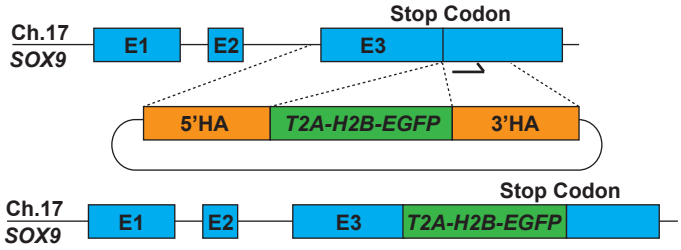

b *SOX9-T2A-H2B-EGFP* organoid

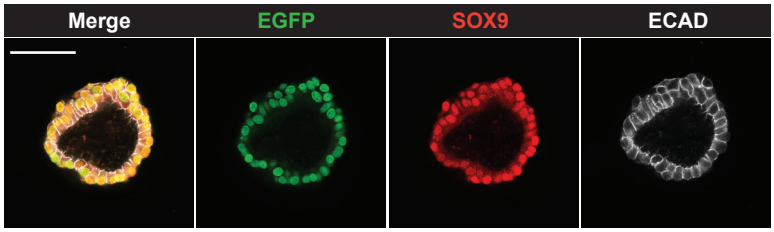

c Reporter design for transcriptionally silent genes

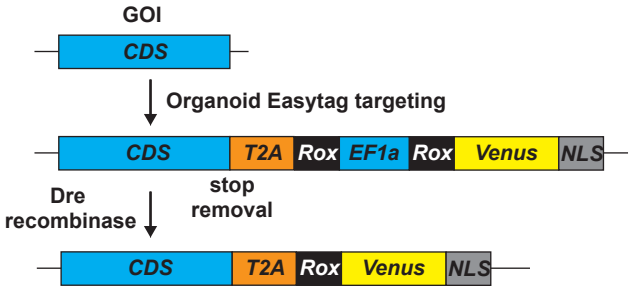

d *SFTPC* reporter design

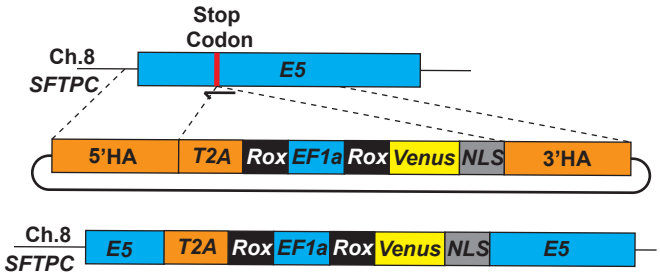

e

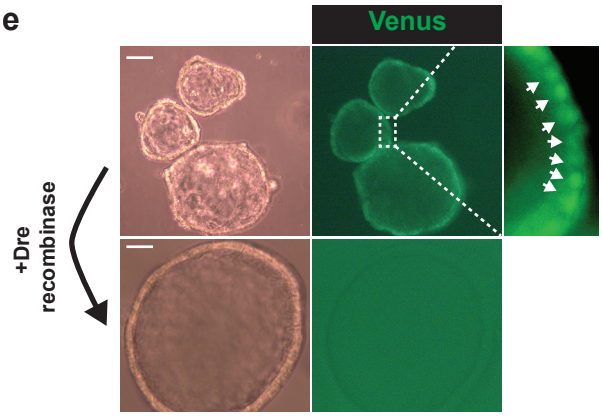

f

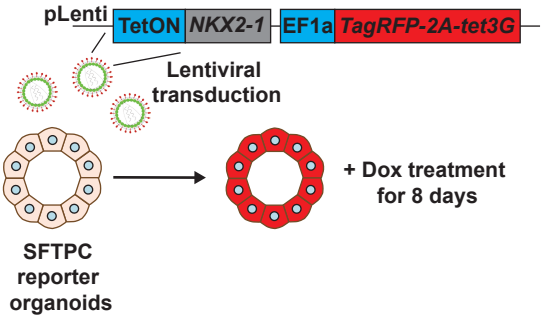

g

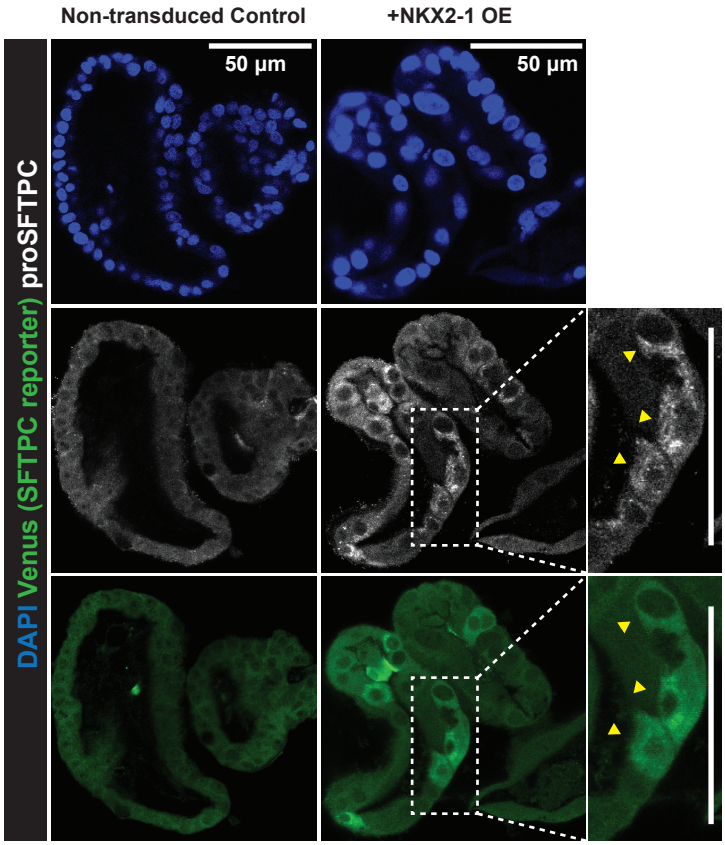

h *SOX2 KO* design

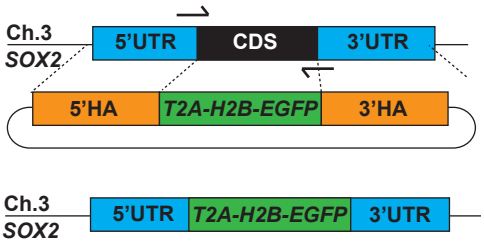

i

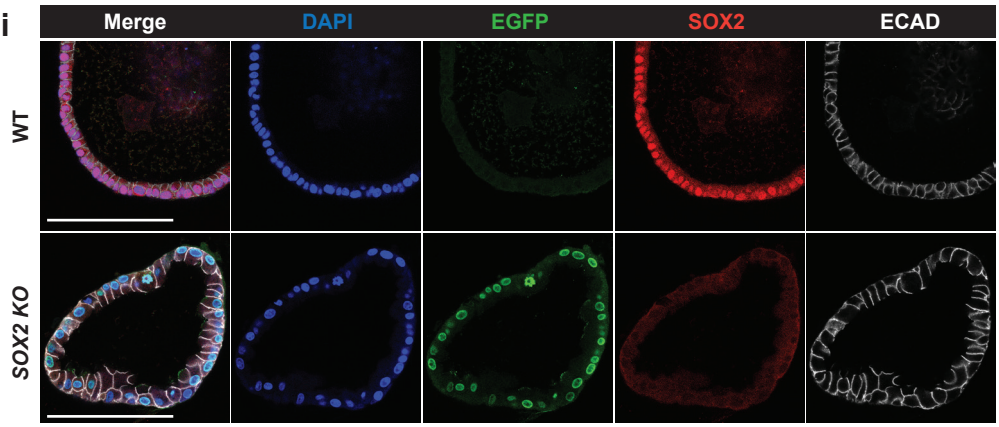

Figure 3. Precise temporal control of CRISPRi in human foetal lung organoids can be achieved via combining the Dox inducible system with a protein destabilising domain.

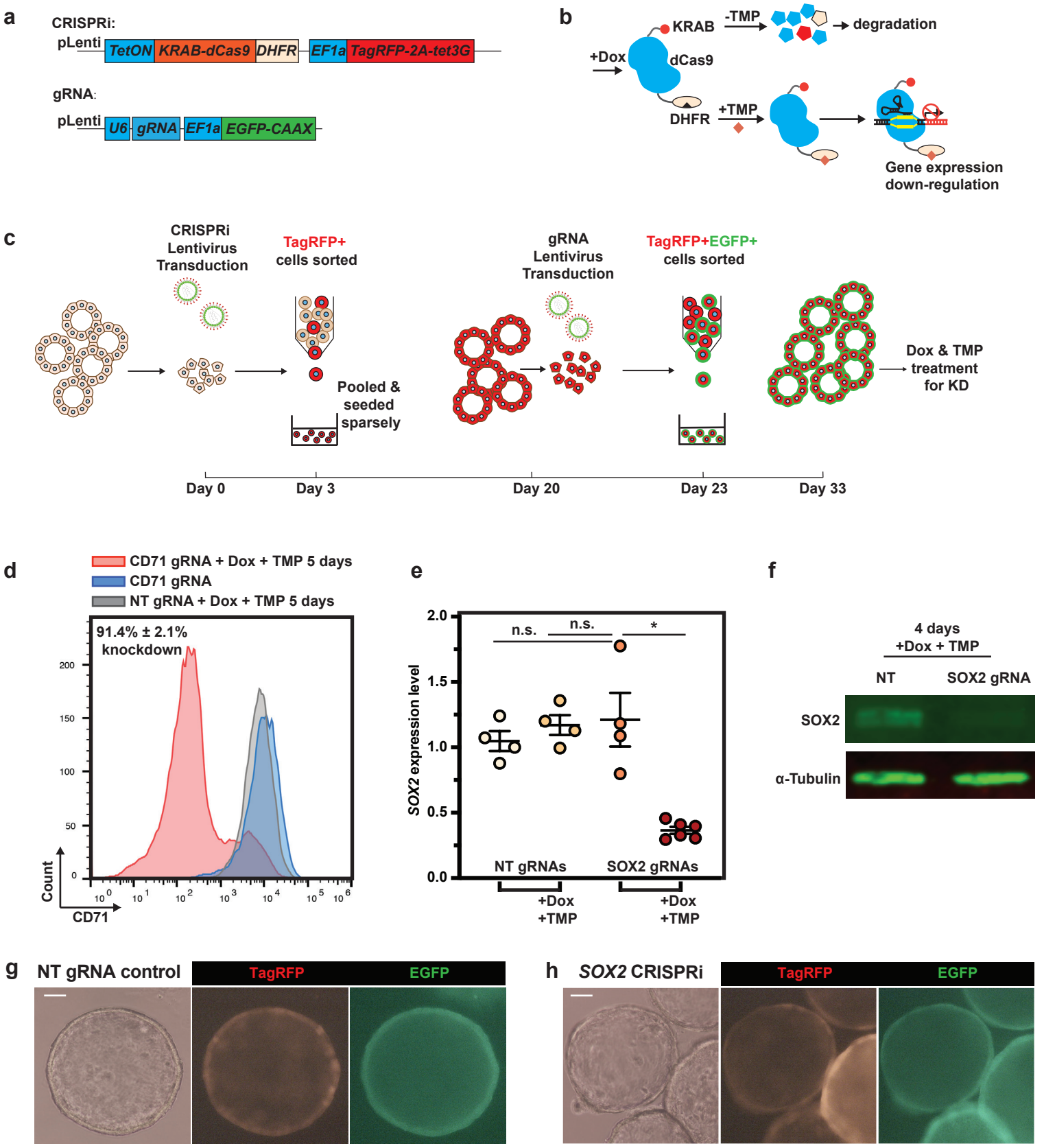

Figure 4. Inducible CRISPRa induced silent gene, *SFTPC*, expression in human foetal lung organoids.

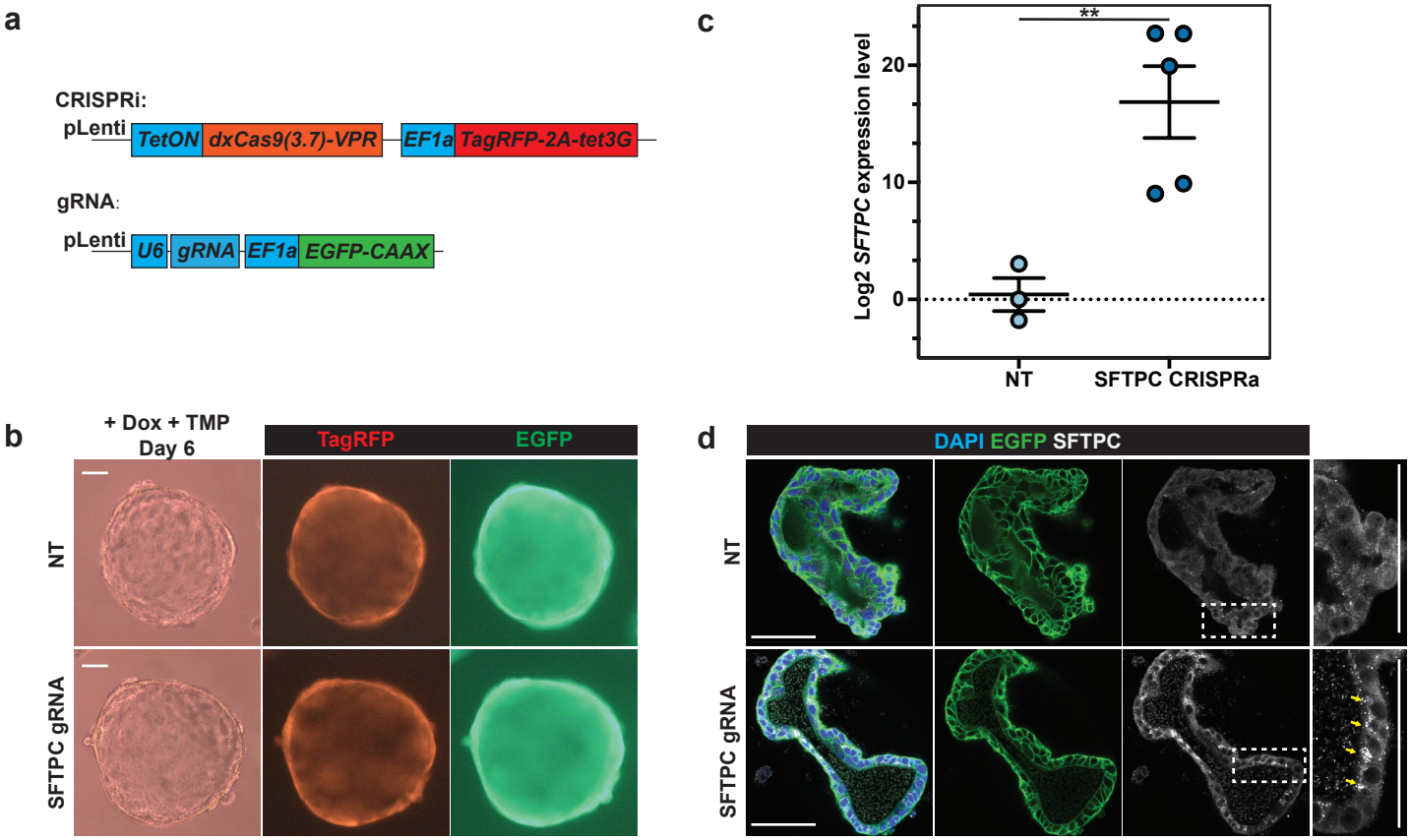

Supplementary Figure 1. Optimisation of DNA delivery and CRISPR/Cas9 site specific DNA cleavage efficiency.

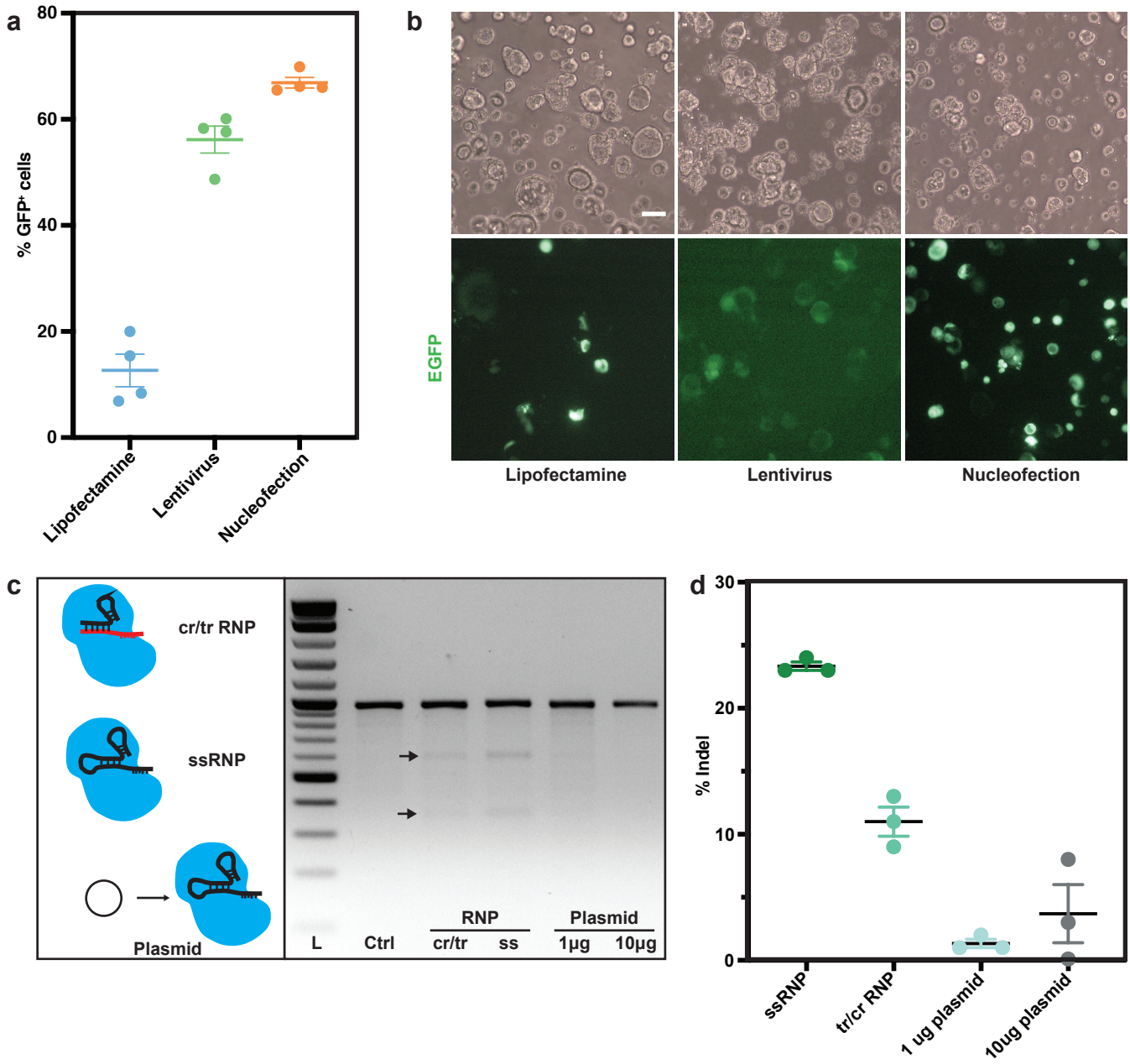

Supplementary Figure 2. Small molecules did not improve organoid gene targeting efficiency.

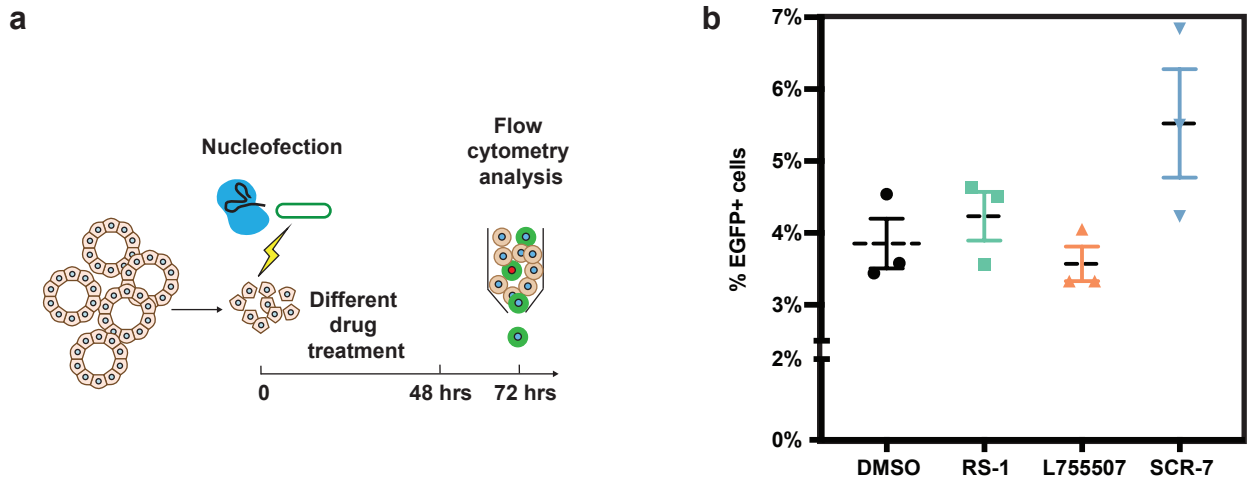

Supplementary Figure 3. Characterisation of *SOX9* targeted colonies.

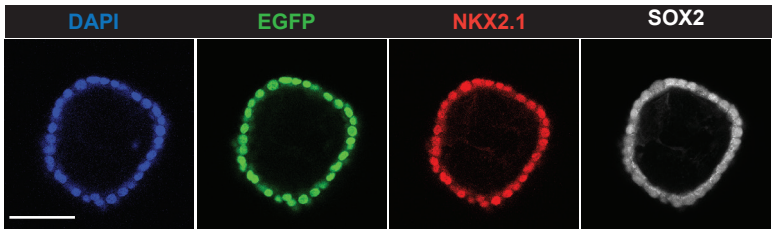

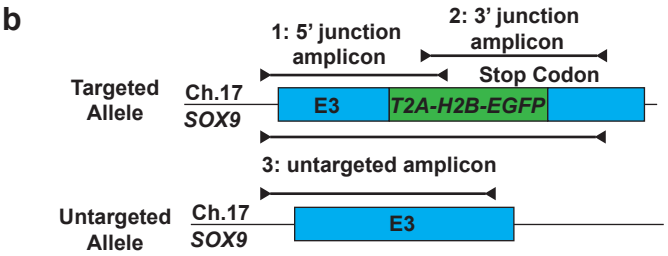

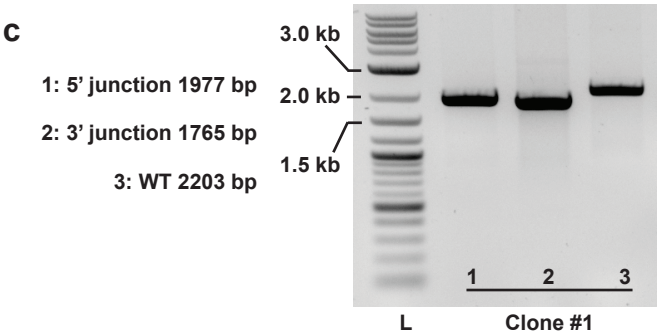

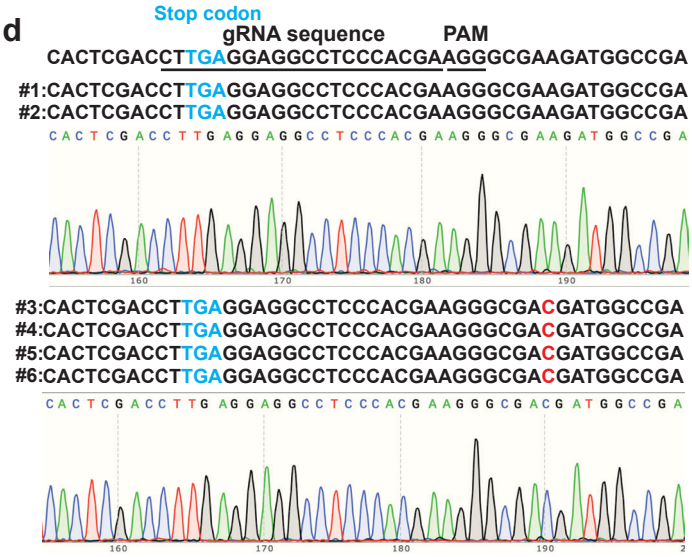

Supplementary Figure 4. Organoid Easytag to target the *SFTPC* locus.

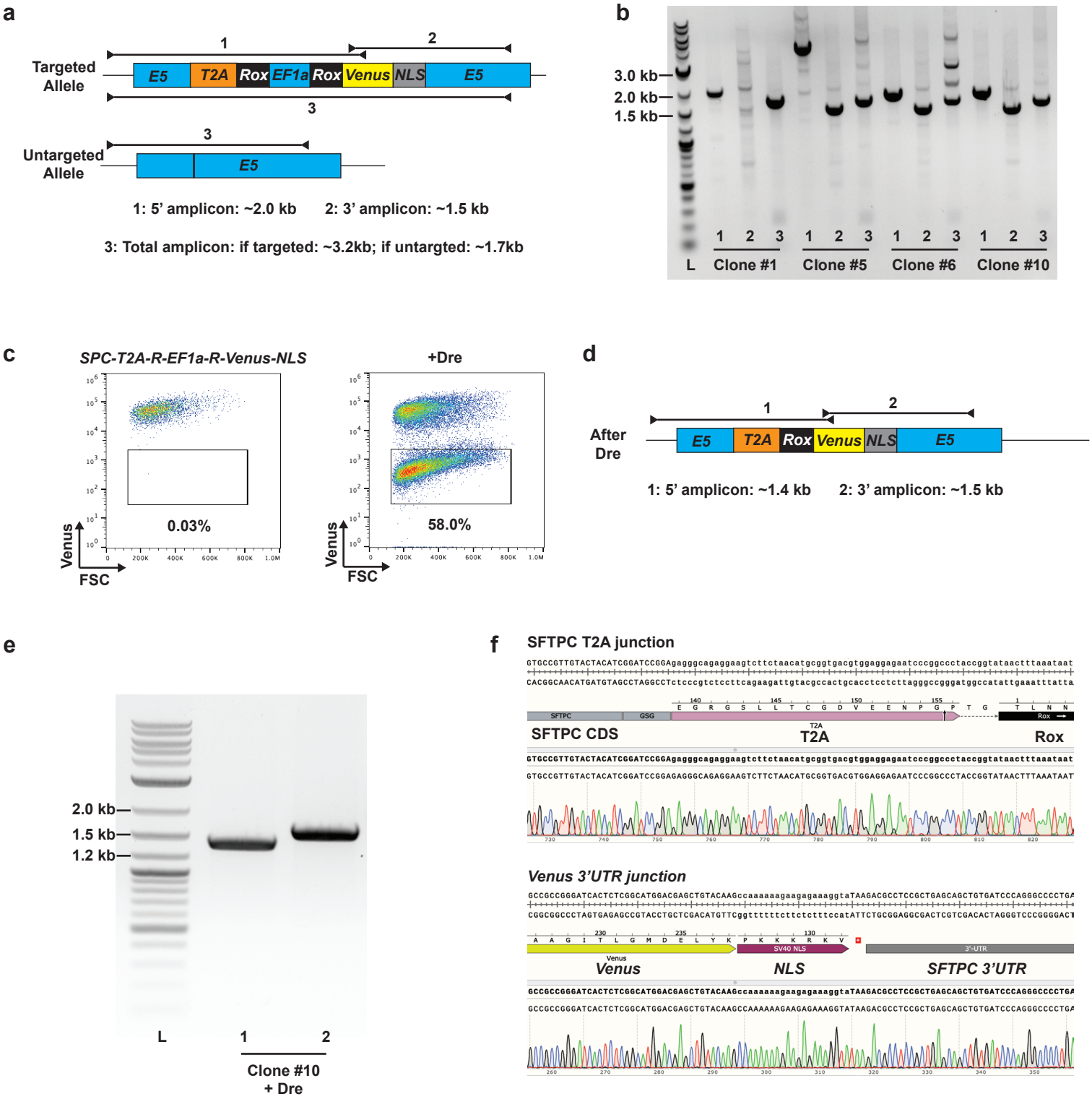

Supplementary Figure 5. Organoid Easytag to target *TP63* locus.

a

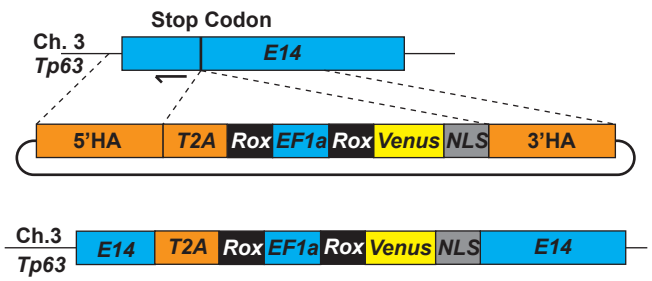

b

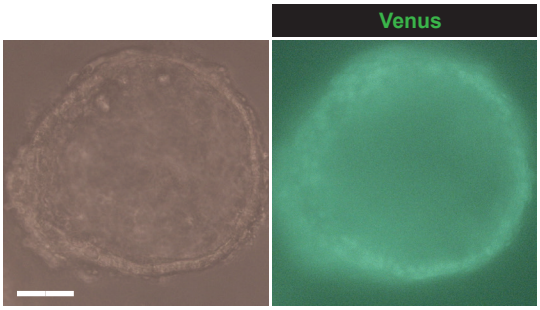

c

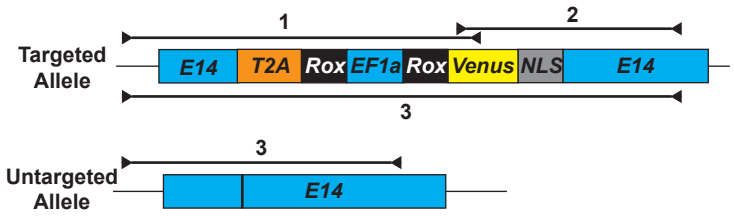

1: 5' amplicon: ~2.1kb 2: 3' amplicon: ~1.6kb

3: Total amplicon: if targeted: ~3.5kb; if untargted: ~2.0kb

d

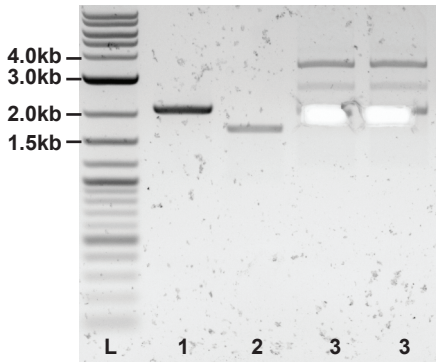

e

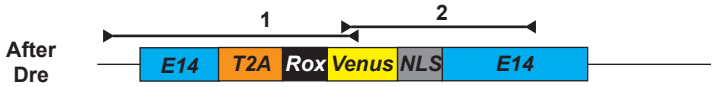

1: 5' amplicon: ~1.5kb 2: 3' amplicon: ~1.7kb

f

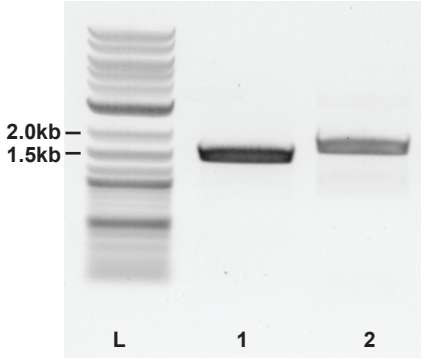

g

Targeting	Number of organoid lines tested	Positive/total colonies genotyped	% of correctly targeted colonies picked
mEGFP-ACTB	2	17/29	59%
SOX9-T2A-H2B-EGFP	3	9/23	39%
AAVS1-EF1α-mTagRFP-T-CAAX	1	4/6	66%
SFTPC reporter	1	1/16 (1)	6.25%
TP63 reporter	2	4/10 (1)	40%

Supplementary Figure 6. Generation of *SOX2* knockout using organoid Easytag workflow.

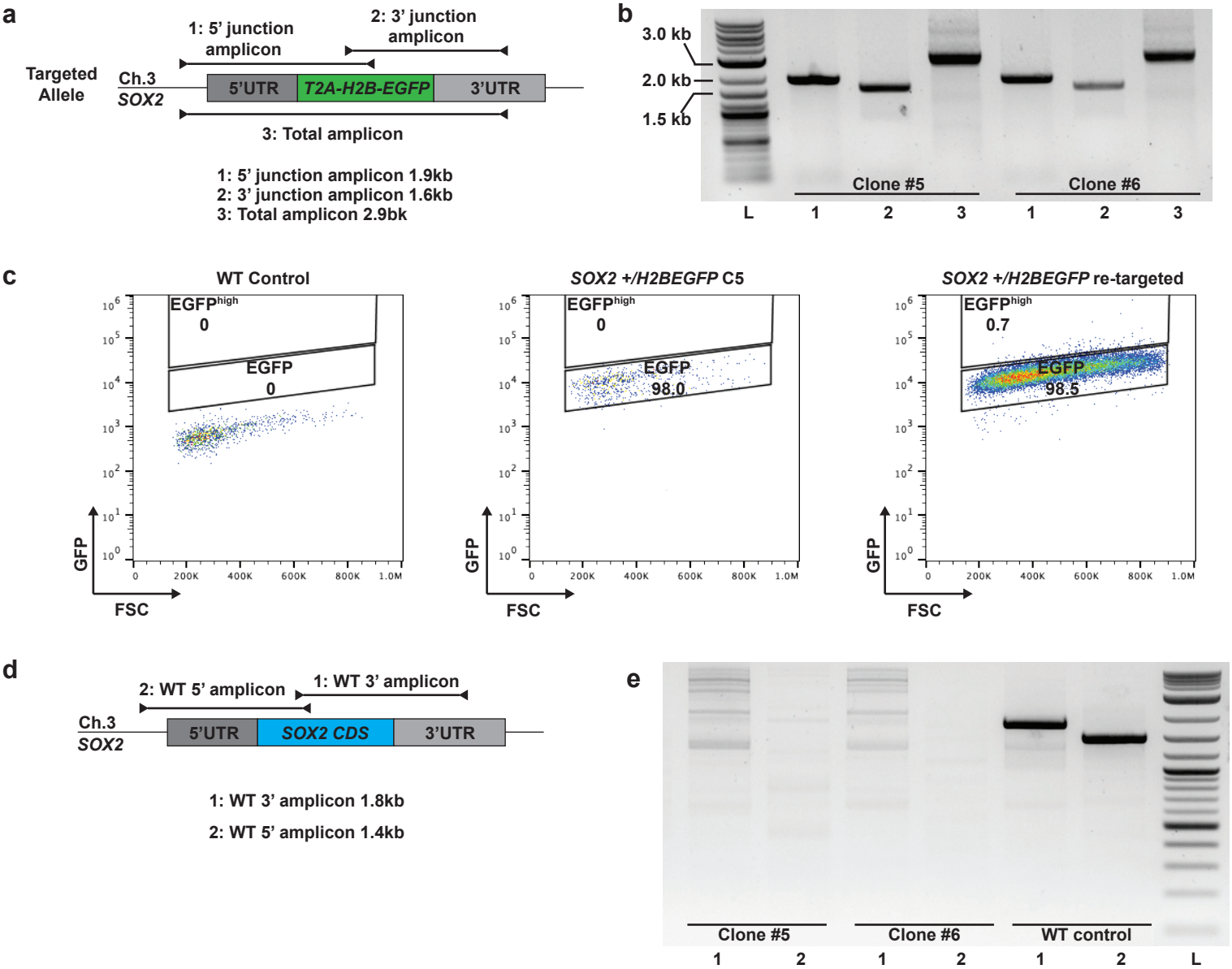

Supplementary Figure 7. TetON system alone was not able to tightly control CRISPRi function.

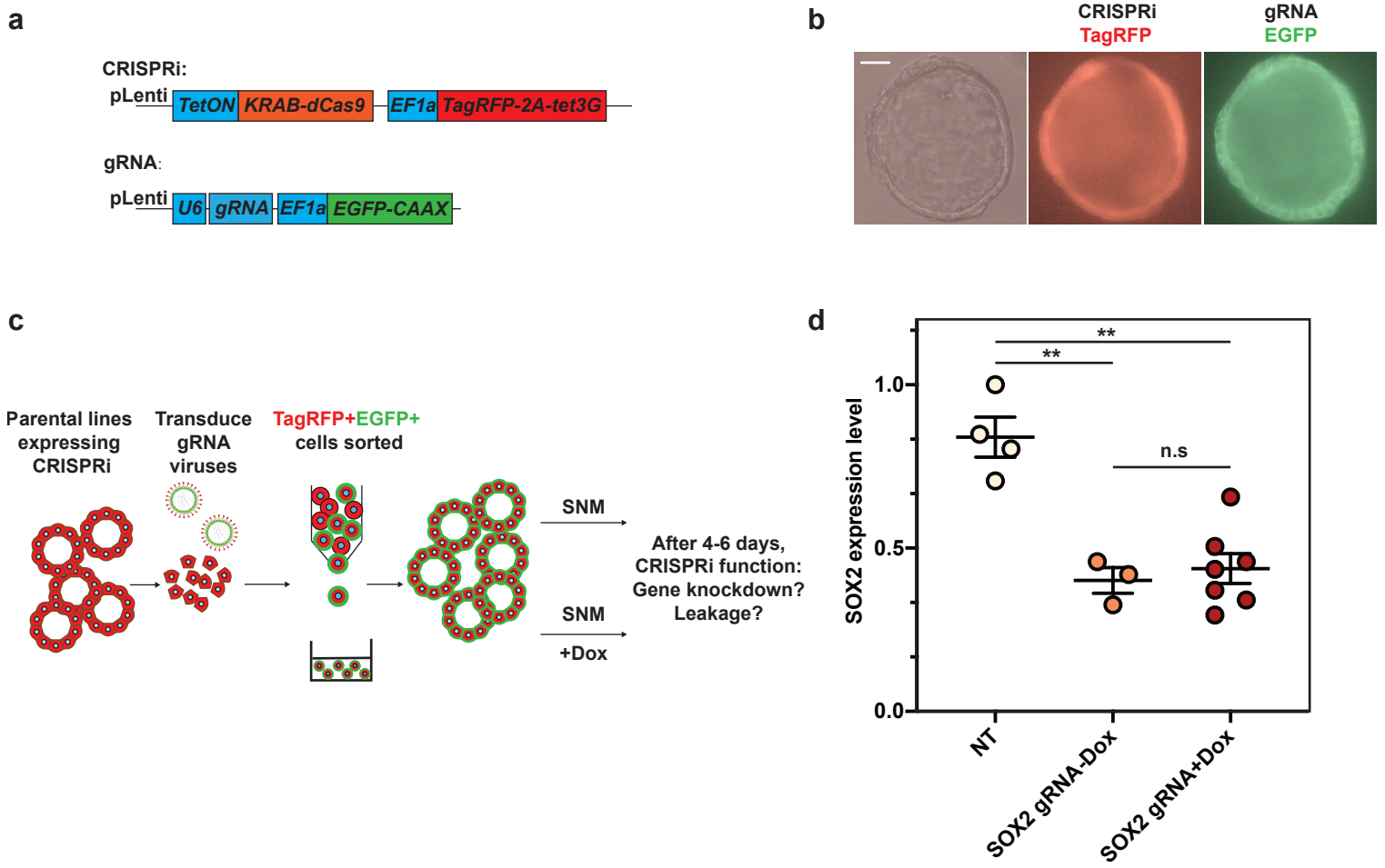
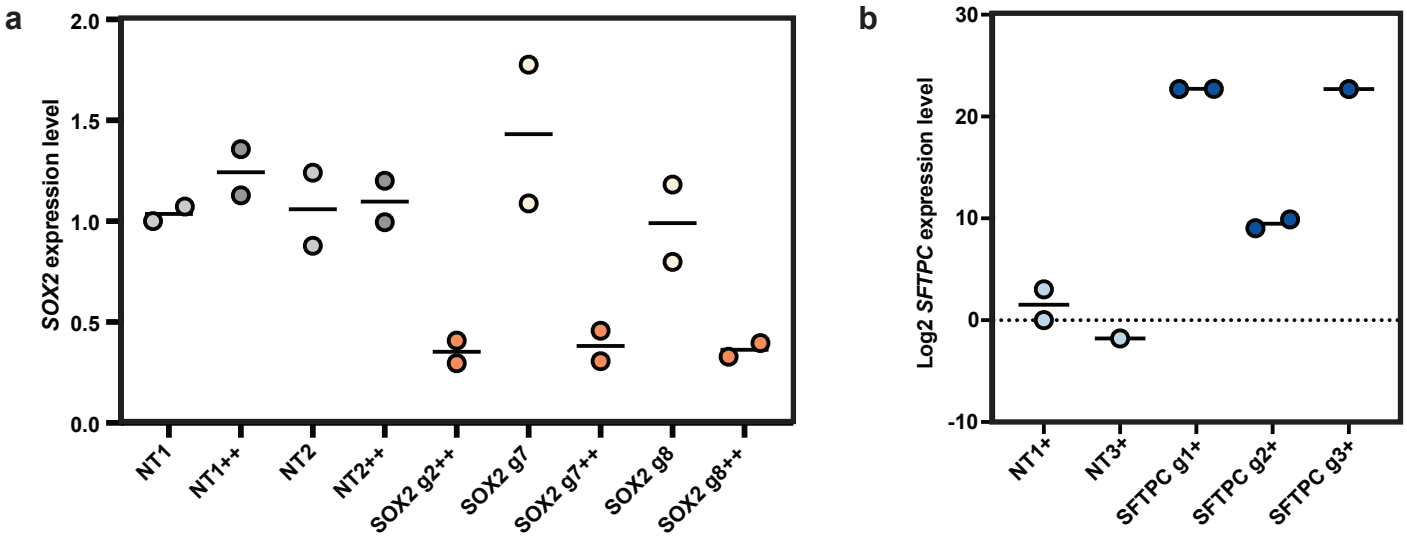
Supplementary Figure 8. SOX2 CRISPRi and SFTPC CRISPRa results break down.